

## 7.1 Introduction

This chapter examines the rotation of rigid bodies (e.g., the planets) in three dimensions. The analysis presented here is largely due to Euler (1707–1783).

## 7.2 Fundamental equations

We can think of a rigid body as a collection of a large number of small mass elements that all maintain a fixed spatial relationship with respect to one another. Let there be  $N$  elements, and let the  $i$ th element be of mass  $m_i$ , and instantaneous position vector  $\mathbf{r}_i$ . The equation of motion of the  $i$ th element is written

$$m_i \frac{d^2 \mathbf{r}_i}{dt^2} = \sum_{j=1,N}^{j \neq i} \mathbf{f}_{ij} + \mathbf{F}_i. \quad (7.1)$$

Here,  $\mathbf{f}_{ij}$  is the internal force exerted on the  $i$ th element by the  $j$ th element, and  $\mathbf{F}_i$  the external force acting on the  $i$ th element. The internal forces  $\mathbf{f}_{ij}$  represent the stresses that develop within the body to ensure that its various elements maintain a fixed spatial relationship with respect to one another. Of course,  $\mathbf{f}_{ij} = -\mathbf{f}_{ji}$ , by Newton's third law. The external forces represent forces that originate outside the body.

Repeating the analysis of Section 1.6, we can sum Equation (7.1) over all mass elements to obtain

$$M \frac{d^2 \mathbf{r}_{cm}}{dt^2} = \mathbf{F}. \quad (7.2)$$

Here,  $M = \sum_{i=1,N} m_i$  is the total mass,  $\mathbf{r}_{cm}$  the position vector of the center of mass [see Equation (1.27)], and  $\mathbf{F} = \sum_{i=1,N} \mathbf{F}_i$  the total external force. It can be seen that the center of mass of a rigid body moves under the action of the external forces like a point particle whose mass is identical with that of the body.

Again repeating the analysis of Section 1.6, we can sum  $\mathbf{r}_i \times$  Equation (7.1) over all mass elements to obtain

$$\frac{d\mathbf{L}}{dt} = \boldsymbol{\tau}. \quad (7.3)$$

Here,  $\mathbf{L} = \sum_{i=1,N} m_i \mathbf{r}_i \times d\mathbf{r}_i/dt$  is the total angular momentum of the body (about the origin), and  $\boldsymbol{\tau} = \sum_{i=1,N} \mathbf{r}_i \times \mathbf{F}_i$  is the total external torque (about the origin). The

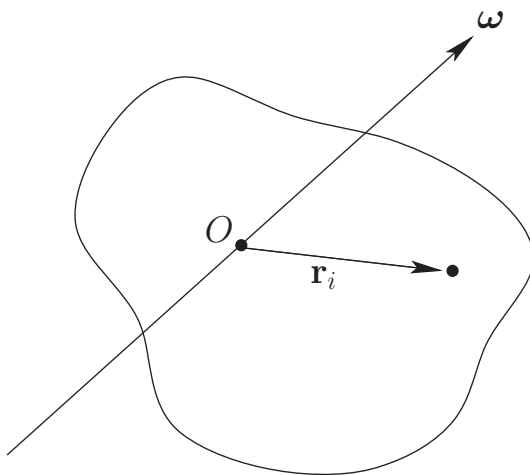


**Fig. 7.1** A rigid rotating body.

preceding equation is valid only if the internal forces are *central* in nature. However, this is not a particularly onerous constraint. Equation (7.3) describes how the angular momentum of a rigid body evolves in time under the action of the external torques.

In the following, we shall consider only the *rotational* motion of rigid bodies, as their translational motion is similar to that of point particles [see Equation (7.2)] and, therefore, is fairly straightforward in nature.

### 7.3 Moment of inertia tensor

Consider a rigid body rotating with fixed angular velocity  $\omega$  about an axis that passes through the origin. (See Figure 7.1.) Let  $\mathbf{r}_i$  be the position vector of the  $i$ th mass element, whose mass is  $m_i$ . We expect this position vector to *precess* about the axis of rotation (which is parallel to  $\omega$ ) with angular velocity  $\omega$ . It, therefore, follows from Section A.7 that

$$\frac{d\mathbf{r}_i}{dt} = \omega \times \mathbf{r}_i. \quad (7.4)$$

Thus, Equation (7.4) specifies the velocity,  $\mathbf{v}_i = d\mathbf{r}_i/dt$ , of each mass element as the body rotates with fixed angular velocity  $\omega$  about an axis passing through the origin.

The total angular momentum of the body (about the origin) is written

$$\mathbf{L} = \sum_{i=1,N} m_i \mathbf{r}_i \times \frac{d\mathbf{r}_i}{dt} = \sum_{i=1,N} m_i \mathbf{r}_i \times (\omega \times \mathbf{r}_i) = \sum_{i=1,N} m_i [r_i^2 \omega - (\mathbf{r}_i \cdot \omega) \mathbf{r}_i], \quad (7.5)$$

where use has been made of Equation (7.4) and some standard vector identities. (See Section A.4.) The preceding formula can be written as a matrix equation of the form

$$\begin{pmatrix} L_x \\ L_y \\ L_z \end{pmatrix} = \begin{pmatrix} \mathcal{I}_{xx} & \mathcal{I}_{xy} & \mathcal{I}_{xz} \\ \mathcal{I}_{yx} & \mathcal{I}_{yy} & \mathcal{I}_{yz} \\ \mathcal{I}_{zx} & \mathcal{I}_{zy} & \mathcal{I}_{zz} \end{pmatrix} \begin{pmatrix} \omega_x \\ \omega_y \\ \omega_z \end{pmatrix}, \quad (7.6)$$

where

$$\mathcal{I}_{xx} = \sum_{i=1,N} (y_i^2 + z_i^2) m_i = \int (y^2 + z^2) dm, \quad (7.7)$$

$$\mathcal{I}_{yy} = \sum_{i=1,N} (x_i^2 + z_i^2) m_i = \int (x^2 + z^2) dm, \quad (7.8)$$

$$\mathcal{I}_{zz} = \sum_{i=1,N} (x_i^2 + y_i^2) m_i = \int (x^2 + y^2) dm, \quad (7.9)$$

$$\mathcal{I}_{xy} = \mathcal{I}_{yx} = - \sum_{i=1,N} x_i y_i m_i = - \int xy dm, \quad (7.10)$$

$$\mathcal{I}_{yz} = \mathcal{I}_{zy} = - \sum_{i=1,N} y_i z_i m_i = - \int yz dm, \quad (7.11)$$

and

$$\mathcal{I}_{xz} = \mathcal{I}_{zx} = - \sum_{i=1,N} x_i z_i m_i = - \int xz dm. \quad (7.12)$$

Here,  $\mathcal{I}_{xx}$  is called the *moment of inertia* about the  $x$ -axis,  $\mathcal{I}_{yy}$  the moment of inertia about the  $y$ -axis,  $\mathcal{I}_{xy}$  the  $xy$  product of inertia,  $\mathcal{I}_{yz}$  the  $yz$  product of inertia, and so on. The matrix of the  $\mathcal{I}_{ij}$  values is known as the *moment of inertia tensor*. Each component of the moment of inertia tensor can be written as either a sum over separate mass elements or as an integral over infinitesimal mass elements. In the integrals,  $dm = \rho d^3\mathbf{r}$ , where  $\rho$  is the mass density, and  $d^3\mathbf{r}$  a volume element. Equation (7.6) can be written more succinctly as

$$\mathbf{L} = \mathbf{I}\boldsymbol{\omega}. \quad (7.13)$$

Here, it is understood that  $\mathbf{L}$  and  $\boldsymbol{\omega}$  are both *column vectors*, and  $\mathbf{I}$  is the *matrix* of the  $\mathcal{I}_{ij}$  values. Note that  $\mathbf{I}$  is a *real symmetric* matrix:  $\mathcal{I}_{ij}^* = \mathcal{I}_{ij}$  and  $\mathcal{I}_{ji} = \mathcal{I}_{ij}$ .

In general, the angular momentum vector,  $\mathbf{L}$ , obtained from Equation (7.13), points in a different direction from the angular velocity vector,  $\boldsymbol{\omega}$ . In other words,  $\mathbf{L}$  is generally not parallel to  $\boldsymbol{\omega}$ .

Finally, although the preceding results were obtained assuming a fixed angular velocity, they remain valid, at each instant in time, if the angular velocity varies.

## 7.4 Rotational kinetic energy

The instantaneous rotational kinetic energy of a rotating rigid body is written

$$K = \frac{1}{2} \sum_{i=1,N} m_i \left( \frac{d\mathbf{r}_i}{dt} \right)^2. \quad (7.14)$$

Making use of Equation (7.4) and some vector identities (see Section A.4), we find that the kinetic energy takes the form

$$K = \frac{1}{2} \sum_{i=1,N} m_i (\boldsymbol{\omega} \times \mathbf{r}_i) \cdot (\boldsymbol{\omega} \times \mathbf{r}_i) = \frac{1}{2} \boldsymbol{\omega} \cdot \sum_{i=1,N} m_i \mathbf{r}_i \times (\boldsymbol{\omega} \times \mathbf{r}_i). \quad (7.15)$$

Hence, it follows from Equation (7.5) that

$$K = \frac{1}{2} \boldsymbol{\omega} \cdot \mathbf{L}. \quad (7.16)$$

Making use of Equation (7.13), we can also write

$$K = \frac{1}{2} \boldsymbol{\omega}^T \mathbf{I} \boldsymbol{\omega}. \quad (7.17)$$

Here,  $\boldsymbol{\omega}^T$  is the *row vector* of the Cartesian components  $\omega_x, \omega_y, \omega_z$ , which is, of course, the transpose (denoted  $T$ ) of the column vector  $\boldsymbol{\omega}$ . When written in component form, Equation (7.17) yields

$$K = \frac{1}{2} \left( \mathcal{I}_{xx} \omega_x^2 + \mathcal{I}_{yy} \omega_y^2 + \mathcal{I}_{zz} \omega_z^2 + 2 \mathcal{I}_{xy} \omega_x \omega_y + 2 \mathcal{I}_{yz} \omega_y \omega_z + 2 \mathcal{I}_{xz} \omega_x \omega_z \right). \quad (7.18)$$

## 7.5 Principal axes of rotation

We have seen that, for a general orientation of the Cartesian coordinate axes, the moment of inertia tensor,  $\mathbf{I}$ , defined in Section 7.3, takes the form of a *real symmetric*  $3 \times 3$  matrix. It therefore follows, from the standard matrix theory discussed in Section A.11, that the moment of inertia tensor possesses three mutually orthogonal eigenvectors, which are associated with three real eigenvalues. Let the  $i$ th eigenvector (which can be normalized to be a unit vector) be denoted  $\hat{\boldsymbol{\omega}}_i$ , and the  $i$ th eigenvalue  $\lambda_i$ . It then follows that

$$\mathbf{I} \hat{\boldsymbol{\omega}}_i = \lambda_i \hat{\boldsymbol{\omega}}_i \quad (7.19)$$

for  $i = 1, 3$ .

The directions of the three mutually orthogonal unit vectors  $\hat{\boldsymbol{\omega}}_i$  define the three so-called *principal axes of rotation* of the rigid body under investigation. These axes are special because when the body rotates about one of them (i.e., when  $\boldsymbol{\omega}$  is parallel to one of them), the angular momentum vector  $\mathbf{L}$  becomes *parallel* to the angular velocity vector  $\boldsymbol{\omega}$ . This can be seen from a comparison of Equation (7.13) with Equation (7.19).

Suppose that we reorient our Cartesian coordinate axes so they coincide with the mutually orthogonal principal axes of rotation. In this new reference frame, the eigenvectors of  $\mathbf{I}$  are the unit vectors,  $\mathbf{e}_x$ ,  $\mathbf{e}_y$ , and  $\mathbf{e}_z$ , and the eigenvalues are the moments of inertia about these axes,  $\mathcal{I}_{xx}$ ,  $\mathcal{I}_{yy}$ , and  $\mathcal{I}_{zz}$ , respectively. These latter quantities are referred to as the *principal moments of inertia*. The products of inertia are all zero in the new reference frame. Hence, in this frame, the moment of inertia tensor takes the form

of a *diagonal* matrix:

$$\mathbf{I} = \begin{pmatrix} \mathcal{I}_{xx} & 0 & 0 \\ 0 & \mathcal{I}_{yy} & 0 \\ 0 & 0 & \mathcal{I}_{zz} \end{pmatrix}. \quad (7.20)$$

Incidentally, it is easy to verify that  $\mathbf{e}_x$ ,  $\mathbf{e}_y$ , and  $\mathbf{e}_z$  are indeed the eigenvectors of this matrix, with the eigenvalues  $\mathcal{I}_{xx}$ ,  $\mathcal{I}_{yy}$ , and  $\mathcal{I}_{zz}$ , respectively, and that  $\mathbf{L} = \mathbf{I}\boldsymbol{\omega}$  is indeed parallel to  $\boldsymbol{\omega}$  whenever  $\boldsymbol{\omega}$  is directed along  $\mathbf{e}_x$ ,  $\mathbf{e}_y$ , or  $\mathbf{e}_z$ .

When expressed in our new coordinate system, Equation (7.13) yields

$$\mathbf{L} = (\mathcal{I}_{xx} \omega_x, \mathcal{I}_{yy} \omega_y, \mathcal{I}_{zz} \omega_z), \quad (7.21)$$

whereas Equation (7.18) reduces to

$$K = \frac{1}{2} (\mathcal{I}_{xx} \omega_x^2 + \mathcal{I}_{yy} \omega_y^2 + \mathcal{I}_{zz} \omega_z^2). \quad (7.22)$$

In conclusion, we may obtain many great simplifications by choosing a coordinate system whose axes coincide with the principal axes of rotation of the rigid body under investigation.

## 7.6 Euler's equations

The fundamental equation of motion of a rotating body [see Equation (7.3)],

$$\boldsymbol{\tau} = \frac{d\mathbf{L}}{dt}, \quad (7.23)$$

is valid only in an *inertial* frame. However, we have seen that  $\mathbf{L}$  is most simply expressed in a frame of reference whose axes are aligned along the principal axes of rotation of the body. Such a frame of reference rotates with the body and is therefore noninertial. Thus, it is helpful to define two Cartesian coordinate systems with the same origins. The first, with coordinates  $x$ ,  $y$ ,  $z$ , is a fixed inertial frame—let us denote this the *fixed frame*. The second, with coordinates  $x'$ ,  $y'$ ,  $z'$ , co-rotates with the body in such a manner that the  $x'$ -,  $y'$ -, and  $z'$ -axes are always pointing along its principal axes of rotation—we shall refer to this as the *body frame*. Because the body frame co-rotates with the body, its instantaneous angular velocity is the same as that of the body. Hence, it follows from the analysis in Section 5.2 that

$$\frac{d\mathbf{L}}{dt} = \frac{d\mathbf{L}}{dt'} + \boldsymbol{\omega} \times \mathbf{L}. \quad (7.24)$$

Here,  $d/dt$  is the time derivative in the fixed frame, and  $d/dt'$  the time derivative in the body frame. Combining Equations (7.23) and (7.24), we obtain

$$\boldsymbol{\tau} = \frac{d\mathbf{L}}{dt'} + \boldsymbol{\omega} \times \mathbf{L}. \quad (7.25)$$

In the body frame, let  $\boldsymbol{\tau} = (\tau_{x'}, \tau_{y'}, \tau_{z'})$  and  $\boldsymbol{\omega} = (\omega_{x'}, \omega_{y'}, \omega_{z'})$ . It follows that  $\mathbf{L} = (\mathcal{I}_{x'x'} \omega_{x'}, \mathcal{I}_{y'y'} \omega_{y'}, \mathcal{I}_{z'z'} \omega_{z'})$ , where  $\mathcal{I}_{x'x'}$ ,  $\mathcal{I}_{y'y'}$ , and  $\mathcal{I}_{z'z'}$  are the principal moments of

inertia. Hence, in the body frame, the components of Equation (7.25) yield

$$\tau_{x'} = \mathcal{I}_{x'x'} \dot{\omega}_{x'} - (\mathcal{I}_{y'y} - \mathcal{I}_{z'z'}) \omega_{y'} \omega_{z'}, \quad (7.26)$$

$$\tau_{y'} = \mathcal{I}_{y'y'} \dot{\omega}_{y'} - (\mathcal{I}_{z'z'} - \mathcal{I}_{x'x'}) \omega_{z'} \omega_{x'}, \quad (7.27)$$

and

$$\tau_{z'} = \mathcal{I}_{z'z'} \dot{\omega}_{z'} - (\mathcal{I}_{x'x'} - \mathcal{I}_{y'y'}) \omega_{x'} \omega_{y'}, \quad (7.28)$$

where  $\dot{\cdot} = d/dt'$ . Here, we have made use of the fact that the moments of inertia of a rigid body are constant in time in the co-rotating body frame. The preceding three equations are known as *Euler's equations*.

Consider a body that is *freely rotating*—that is, in the absence of external torques. Furthermore, let the body be *rotationally symmetric* about the  $z'$ -axis. It follows that  $\mathcal{I}_{x'x'} = \mathcal{I}_{y'y'} = \mathcal{I}_\perp$ . Likewise, we can write  $\mathcal{I}_{z'z'} = \mathcal{I}_\parallel$ . In general, however,  $\mathcal{I}_\perp \neq \mathcal{I}_\parallel$ . Thus, Euler's equations yield

$$\mathcal{I}_\perp \frac{d\omega_{x'}}{dt'} + (\mathcal{I}_\parallel - \mathcal{I}_\perp) \omega_{z'} \omega_{y'} = 0, \quad (7.29)$$

$$\mathcal{I}_\perp \frac{d\omega_{y'}}{dt'} - (\mathcal{I}_\parallel - \mathcal{I}_\perp) \omega_{z'} \omega_{x'} = 0, \quad (7.30)$$

and

$$\frac{d\omega_{z'}}{dt'} = 0. \quad (7.31)$$

Clearly,  $\omega_{z'}$  is a constant of the motion. Equations (7.29) and (7.30) can be written

$$\frac{d\omega_{x'}}{dt'} + \mathcal{Q} \omega_{y'} = 0 \quad (7.32)$$

and

$$\frac{d\omega_{y'}}{dt'} - \mathcal{Q} \omega_{x'} = 0, \quad (7.33)$$

where  $\mathcal{Q} = (\mathcal{I}_\parallel/\mathcal{I}_\perp - 1) \omega_{z'}$ . As is easily demonstrated, the solution to these equations is

$$\omega_{x'} = \omega_\perp \cos(\mathcal{Q} t') \quad (7.34)$$

and

$$\omega_{y'} = \omega_\perp \sin(\mathcal{Q} t'), \quad (7.35)$$

where  $\omega_\perp$  is a constant. Thus, the projection of the angular velocity vector onto the  $x'-y'$  plane has the fixed length  $\omega_\perp$ , and rotates steadily about the  $z'$ -axis with angular velocity  $\mathcal{Q}$ . It follows that the length of the angular velocity vector,  $\omega = (\omega_{x'}^2 + \omega_{y'}^2 + \omega_{z'}^2)^{1/2}$ , is a constant of the motion. Clearly, the angular velocity vector subtends some constant angle,  $\alpha$ , with the  $z'$ -axis, which implies that  $\omega_{z'} = \omega \cos \alpha$  and  $\omega_\perp = \omega \sin \alpha$ . Hence, the components of the angular velocity vector are

$$\omega_{x'} = \omega \sin \alpha \cos(\mathcal{Q} t'), \quad (7.36)$$

$$\omega_{y'} = \omega \sin \alpha \sin(\mathcal{Q} t'), \quad (7.37)$$

and

$$\omega_{z'} = \omega \cos \alpha, \quad (7.38)$$

where

$$\Omega = \omega \cos \alpha \left( \frac{\mathcal{I}_{\perp}}{\mathcal{I}_{\parallel}} - 1 \right). \quad (7.39)$$

We conclude that, in the body frame, the angular velocity vector *precesses* about the symmetry axis (i.e., the  $z'$ -axis) with the angular frequency  $\Omega$ . The components of the angular momentum vector are

$$L_{x'} = \mathcal{I}_{\perp} \omega \sin \alpha \cos(\Omega t'), \quad (7.40)$$

$$L_{y'} = \mathcal{I}_{\perp} \omega \sin \alpha \sin(\Omega t'), \quad (7.41)$$

and

$$L_{z'} = \mathcal{I}_{\parallel} \omega \cos \alpha. \quad (7.42)$$

Thus, in the body frame, the angular momentum vector is also of constant length, and precesses about the symmetry axis with the angular frequency  $\Omega$ . Furthermore, the angular momentum vector subtends a constant angle  $\theta$  with the symmetry axis, where

$$\tan \theta = \frac{\mathcal{I}_{\perp}}{\mathcal{I}_{\parallel}} \tan \alpha. \quad (7.43)$$

The angular momentum vector, the angular velocity vector, and the symmetry axis all lie in the same plane, that is,  $\mathbf{e}_{z'} \cdot \mathbf{L} \times \boldsymbol{\omega} = 0$ , as can easily be verified. Moreover, the angular momentum vector lies between the angular velocity vector and the symmetry axis (i.e.,  $\theta < \alpha$ ) for a flattened (or oblate) body (i.e.,  $\mathcal{I}_{\perp} < \mathcal{I}_{\parallel}$ ), whereas the angular velocity vector lies between the angular momentum vector and the symmetry axis (i.e.,  $\theta > \alpha$ ) for an elongated (or prolate) body (i.e.,  $\mathcal{I}_{\perp} > \mathcal{I}_{\parallel}$ ). (See Figure 7.2.)

## 7.7 Euler angles

We have seen how we can solve Euler's equations to determine the properties of a rotating body in the co-rotating body frame. Let us now investigate how we can determine the same properties in the inertial *fixed frame*.

The fixed frame and the body frame share the same origin. Hence, we can transform from one to the other by means of an appropriate rotation of our coordinate axes. In general, if we restrict ourselves to rotations about one of the Cartesian axes, three successive rotations are required to transform the fixed frame into the body frame. There are, in fact, many different ways to combine three successive rotations to achieve this goal. In the following, we shall describe the most widely used method, which is due to Euler.

We start in the fixed frame, which has coordinates  $x$ ,  $y$ ,  $z$ , and unit vectors  $\mathbf{e}_x$ ,  $\mathbf{e}_y$ ,  $\mathbf{e}_z$ . Our first rotation is counterclockwise (if we look down the axis) through an angle  $\phi$

about the  $z$ -axis. The new frame has coordinates  $x'', y'', z''$  and unit vectors  $\mathbf{e}_{x''}$ ,  $\mathbf{e}_{y''}$ ,  $\mathbf{e}_{z''}$ . According to Section A.6, the transformation of coordinates can be represented as follows:

$$\begin{pmatrix} x'' \\ y'' \\ z'' \end{pmatrix} = \begin{pmatrix} \cos \phi & \sin \phi & 0 \\ -\sin \phi & \cos \phi & 0 \\ 0 & 0 & 1 \end{pmatrix} \begin{pmatrix} x \\ y \\ z \end{pmatrix}. \quad (7.44)$$

The angular velocity vector associated with  $\phi$  has the magnitude  $\dot{\phi}$  and is directed along  $\mathbf{e}_z$  (i.e., along the axis of rotation). Hence, we can write

$$\boldsymbol{\omega}_\phi = \dot{\phi} \mathbf{e}_z. \quad (7.45)$$

Clearly,  $\dot{\phi}$  is the precession rate about the  $z$ -axis, as seen in the fixed frame.

The second rotation is counterclockwise (if we look down the axis) through an angle  $\theta$  about the  $x''$ -axis. The new frame has coordinates  $x''', y''', z'''$  and unit vectors  $\mathbf{e}_{x'''}$ ,  $\mathbf{e}_{y'''}$ ,  $\mathbf{e}_{z'''}$ . By analogy with Equation (7.44), the transformation of coordinates can be represented as follows:

$$\begin{pmatrix} x''' \\ y''' \\ z''' \end{pmatrix} = \begin{pmatrix} 1 & 0 & 0 \\ 0 & \cos \theta & \sin \theta \\ 0 & -\sin \theta & \cos \theta \end{pmatrix} \begin{pmatrix} x'' \\ y'' \\ z'' \end{pmatrix}. \quad (7.46)$$

The angular velocity vector associated with  $\theta$  has the magnitude  $\dot{\theta}$  and is directed along  $\mathbf{e}_{x''}$  (i.e., along the axis of rotation). Hence, we can write

$$\boldsymbol{\omega}_\theta = \dot{\theta} \mathbf{e}_{x''}. \quad (7.47)$$

The third rotation is counterclockwise (if we look down the axis) through an angle  $\psi$  about the  $z'''$ -axis. The new frame is the body frame, which has coordinates  $x', y', z'$  and unit vectors  $\mathbf{e}_{x'}$ ,  $\mathbf{e}_{y'}$ ,  $\mathbf{e}_{z'}$ . The transformation of coordinates can be represented as follows:

$$\begin{pmatrix} x' \\ y' \\ z' \end{pmatrix} = \begin{pmatrix} \cos \psi & \sin \psi & 0 \\ -\sin \psi & \cos \psi & 0 \\ 0 & 0 & 1 \end{pmatrix} \begin{pmatrix} x''' \\ y''' \\ z''' \end{pmatrix}. \quad (7.48)$$

The angular velocity vector associated with  $\psi$  has the magnitude  $\dot{\psi}$  and is directed along  $\mathbf{e}_{z''}$  (i.e., along the axis of rotation). Note that  $\mathbf{e}_{z'''} = \mathbf{e}_{z'}$ , since the third rotation is about  $\mathbf{e}_{z'''}$ . Hence, we can write

$$\boldsymbol{\omega}_\psi = \dot{\psi} \mathbf{e}_{z'}. \quad (7.49)$$

Clearly,  $\dot{\psi}$  is *minus* the precession rate about the  $z'$ -axis, as seen in the body frame.

The full transformation between the fixed frame and the body frame is rather complicated. However, the following results can easily be verified:

$$\mathbf{e}_z = \sin \psi \sin \theta \mathbf{e}_{x'} + \cos \psi \sin \theta \mathbf{e}_{y'} + \cos \theta \mathbf{e}_{z'}, \quad (7.50)$$

$$\mathbf{e}_{x''} = \cos \psi \mathbf{e}_{x'} - \sin \psi \mathbf{e}_{y'}. \quad (7.51)$$

It follows from Equation (7.50) that  $\mathbf{e}_z \cdot \mathbf{e}_{z'} = \cos \theta$ . In other words,  $\theta$  is the angle of inclination between the  $z$ - and  $z'$ -axes. Finally, because the total angular velocity can be

written

$$\boldsymbol{\omega} = \boldsymbol{\omega}_\phi + \boldsymbol{\omega}_\theta + \boldsymbol{\omega}_\psi, \quad (7.52)$$

Equations (7.45), (7.47), and (7.49)–(7.51) yield

$$\omega_{x'} = \sin \psi \sin \theta \dot{\phi} + \cos \psi \dot{\theta}, \quad (7.53)$$

$$\omega_{y'} = \cos \psi \sin \theta \dot{\phi} - \sin \psi \dot{\theta}, \quad (7.54)$$

and

$$\omega_{z'} = \cos \theta \dot{\phi} + \dot{\psi}. \quad (7.55)$$

The angles  $\phi$ ,  $\theta$ , and  $\psi$  are termed *Euler angles*. Each has a clear physical interpretation:  $\phi$  is the angle of precession about the  $z$ -axis in the fixed frame,  $\psi$  is minus the angle of precession about the  $z'$ -axis in the body frame, and  $\theta$  is the angle of inclination between the  $z$ - and  $z'$ -axes. Moreover, we can express the components of the angular velocity vector  $\boldsymbol{\omega}$  in the body frame entirely in terms of the Eulerian angles and their time derivatives [see Equations (7.53)–(7.55)].

Consider a freely rotating body that is rotationally symmetric about one axis (the  $z'$ -axis). In the absence of an external torque, the angular momentum vector  $\mathbf{L}$  is a constant of the motion [see Equation (7.3)]. Let  $\mathbf{L}$  point along the  $z$ -axis. In the previous section, we saw that the angular momentum vector subtends a constant angle  $\theta$  with the axis of symmetry, that is, with the  $z'$ -axis. Hence, the time derivative of the Eulerian angle  $\theta$  is zero. We also saw that the angular momentum vector, the axis of symmetry, and the angular velocity vector are coplanar. Consider an instant in time at which all these vectors lie in the  $y'-z'$  plane. This implies that  $\omega_{x'} = 0$ . According to the previous section, the angular velocity vector subtends a constant angle  $\alpha$  with the symmetry axis. It follows that  $\omega_y = \omega \sin \alpha$  and  $\omega_{z'} = \omega \cos \alpha$ . Equation (7.53) gives  $\psi = 0$ . Hence, Equation (7.54) yields

$$\omega \sin \alpha = \sin \theta \dot{\phi}. \quad (7.56)$$

This can be combined with Equation (7.43) to give

$$\dot{\phi} = \omega \left[ 1 + \left( \frac{\mathcal{I}_{\parallel}^2}{\mathcal{I}_{\perp}^2} - 1 \right) \cos^2 \alpha \right]^{1/2}. \quad (7.57)$$

Finally, Equation (7.55), together with Equations (7.43) and (7.56), yields

$$\dot{\psi} = \omega \cos \alpha - \cos \theta \dot{\phi} = \omega \cos \alpha \left( 1 - \frac{\tan \alpha}{\tan \theta} \right) = \omega \cos \alpha \left( 1 - \frac{\mathcal{I}_{\parallel}}{\mathcal{I}_{\perp}} \right). \quad (7.58)$$

A comparison of this equation with Equation (7.39) gives

$$\dot{\psi} = -\Omega. \quad (7.59)$$

Thus, as expected,  $\dot{\psi}$  is minus the precession rate (of the angular momentum and angular velocity vectors) in the body frame. On the other hand,  $\dot{\phi}$  is the precession rate (of the angular velocity vector and the symmetry axis) in the fixed frame. Note that  $\dot{\phi}$  and  $\Omega$  are quite dissimilar. For instance,  $\Omega$  is negative for elongated bodies ( $\mathcal{I}_{\parallel} < \mathcal{I}_{\perp}$ ) whereas  $\dot{\phi}$  is positive definite. It follows that the precession is always in the same sense as  $L_z$  in the

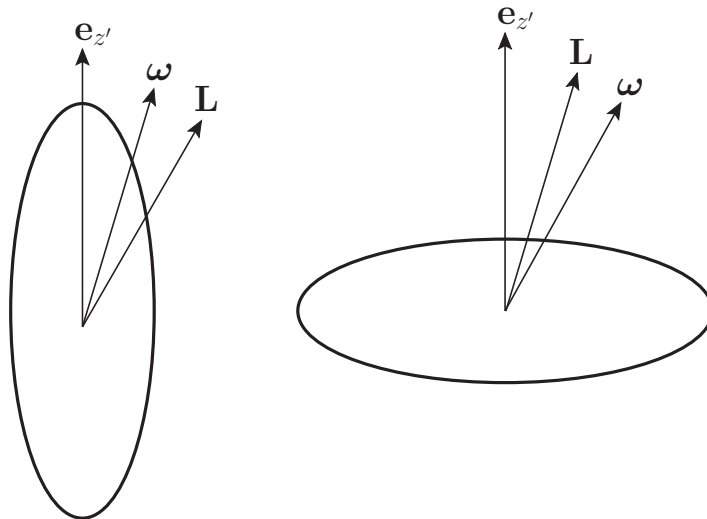


**Fig. 7.2** A freely rotating object that is elongated along its axis of symmetry,  $\mathbf{e}_{z'}$  (left), and a freely rotating object that is flattened along its axis of symmetry (right). The  $\mathbf{L}$  vector is fixed.

fixed frame, whereas the precession in the body frame is in the opposite sense to  $L_{z'}$  for elongated bodies. We found, in the previous section, that for a flattened body the angular momentum vector lies between the angular velocity vector and the symmetry axis. This means that, in the fixed frame, the angular velocity vector and the symmetry axis lie on opposite sides of the fixed angular momentum vector, about which they precess. (See Figure 7.2.) On the other hand, for an elongated body we found that the angular velocity vector lies between the angular momentum vector and the symmetry axis. This means that, in the fixed frame, the angular velocity vector and the symmetry axis lie on the *same* side of the fixed angular momentum vector, about which they precess. (See Figure 7.2.) Recall that the angular momentum vector, the angular velocity vector, and the symmetry axis are coplanar.

## 7.8 Free precession of the Earth

It is known that the Earth's axis of rotation is very slightly inclined to its symmetry axis (which passes through the two geographic poles). The angle  $\alpha$  is approximately 0.2 seconds of an arc (which corresponds to a distance of about 6 m on the Earth's surface). It is also known that the ratio of the terrestrial moments of inertia is about  $\mathcal{I}_{\parallel}/\mathcal{I}_{\perp} = 1.00327$ , as determined from the Earth's oblateness (Yoder 1995). (See Section 7.9.) Hence, from Equation (7.39), the precession rate of the angular velocity vector about the symmetry axis, as viewed in a geostationary reference frame, is

$$\Omega = 0.00327 \omega, \quad (7.60)$$

giving a precession period of

$$T' = \frac{2\pi}{\Omega} = 305 \text{ days.} \quad (7.61)$$

[Of course,  $2\pi/\omega = 1$  (sidereal) day.] The observed period of precession is about 434 days (Yoder 1995). The disagreement between theory and observation is attributed to the fact that the Earth is not perfectly rigid (Bertotti et al. 2003). The Earth's symmetry axis subtends an angle  $\theta \approx \alpha = 0.2''$  [see Equation (7.43)] with its angular momentum vector, but it lies on the opposite side of this vector to the angular velocity vector. This implies that, as viewed from space, the Earth's angular velocity vector is almost parallel to its fixed angular momentum vector, whereas its symmetry axis subtends an angle of  $0.2''$  with both vectors and precesses about them. The (theoretical) precession rate of the Earth's symmetry axis, as seen from space, is given by Equation (7.57):

$$\dot{\phi} = 1.00327 \omega. \quad (7.62)$$

The associated precession period is

$$T = \frac{2\pi}{\dot{\phi}} = 0.997 \text{ days.} \quad (7.63)$$

The free precession of the Earth's symmetry axis in space, which is known as the *Chandler wobble*—because it was discovered by the American astronomer S.C. Chandler (1846–1913) in 1891—is superimposed on a much slower forced precession, with a period of about 26,000 years, caused by the small gravitational torque exerted on the Earth by the Sun and Moon, as a consequence of the Earth's slight oblateness. (See Section 7.10.)

## 7.9 MacCullagh's formula

According to Equations (2.59) and (2.64), if the Earth is modeled as spheroid of uniform density  $\gamma$ , its ellipticity is given by

$$\epsilon = - \int r^2 \gamma P_2(\cos \theta) d^3 \mathbf{r} \Big/ \mathcal{I}_0 = - \frac{1}{2} \int r^2 \gamma (3 \cos^2 \theta - 1) d^3 \mathbf{r} \Big/ \mathcal{I}_0, \quad (7.64)$$

where the integral is over the whole volume of the Earth, and  $\mathcal{I}_0 = (2/5) M R^2$  would be the Earth's moment of inertia were it exactly spherical. The Earth's moment of inertia about its axis of rotation is given by

$$\mathcal{I}_{\parallel} = \int (x^2 + y^2) \gamma d^3 \mathbf{r} = \int r^2 \gamma (1 - \cos^2 \theta) d^3 \mathbf{r}. \quad (7.65)$$

Here, use has been made of Equations (2.24)–(2.26). Likewise, the Earth's moment of inertia about an axis perpendicular to its axis of rotation (and passing through the Earth's

center) is

$$\begin{aligned}\mathcal{I}_{\perp} &= \int (y^2 + z^2) \gamma d^3\mathbf{r} = \int r^2 \gamma (\sin^2 \theta \sin^2 \phi + \cos^2 \theta) d^3\mathbf{r} \\ &= \int r^2 \gamma \left( \frac{1}{2} \sin^2 \theta + \cos^2 \theta \right) d^3\mathbf{r} = \frac{1}{2} \int r^2 \gamma (1 + \cos^2 \theta) d^3\mathbf{r},\end{aligned}\quad (7.66)$$

as the average of  $\sin^2 \phi$  is  $1/2$  for an axisymmetric mass distribution. It follows from the preceding three equations that

$$\epsilon = \frac{\mathcal{I}_{\parallel} - \mathcal{I}_{\perp}}{\mathcal{I}_0} \simeq \frac{\mathcal{I}_{\parallel} - \mathcal{I}_{\perp}}{\mathcal{I}_{\parallel}}.\quad (7.67)$$

This formula demonstrates that the Earth's ellipticity is directly related to the difference between its principal moments of inertia. Actually, the formula holds for *any* axially symmetric mass distribution, not just a spheroidal distribution of uniform density (this is discussed later). When Equation (7.67) is combined with Equation (2.65), we get

$$\Phi(r, \theta) \simeq -\frac{GM}{r} + \frac{G(\mathcal{I}_{\parallel} - \mathcal{I}_{\perp})}{r^3} P_2(\cos \theta),\quad (7.68)$$

which is the general expression for the gravitational potential generated outside an axially symmetric mass distribution. The first term on the right-hand side is the *monopole* gravitational potential that would be generated if all the mass in the distribution were concentrated at its center of mass, whereas the second term is the *quadrupole* potential generated by any deviation from spherical symmetry in the distribution.

More generally, consider an asymmetric mass distribution consisting of  $N$  mass elements. Suppose that the  $i$ th element has mass  $m_i$  and position vector  $\mathbf{r}_i$ , where  $i$  runs from 1 to  $N$ . Let us define a Cartesian coordinate system  $x, y, z$  such that the origin coincides with the center of mass of the distribution. It follows that

$$\sum_{i=1,N} m_i x_i = \sum_{i=1,N} m_i y_i = \sum_{i=1,N} m_i z_i = 0.\quad (7.69)$$

Suppose that the  $x$ -,  $y$ -, and  $z$ -axes coincide with the mass distribution's principal axes of rotation (for rotation about an axis that passes through the origin). It follows from Section 7.5 that

$$\sum_{i=1,N} m_i y_i z_i = \sum_{i=1,N} m_i x_i z_i = \sum_{i=1,N} m_i x_i y_i = 0,\quad (7.70)$$

and that the distribution's principal moments of inertia about the  $x$ -,  $y$ -, and  $z$ -axes take the form

$$\mathcal{I}_{xx} = \sum_{i=1,N} m_i (y_i^2 + z_i^2),\quad (7.71)$$

$$\mathcal{I}_{yy} = \sum_{i=1,N} m_i (x_i^2 + z_i^2),\quad (7.72)$$

and

$$\mathcal{I}_{zz} = \sum_{i=1,N} m_i (x_i^2 + y_i^2),\quad (7.73)$$

respectively.

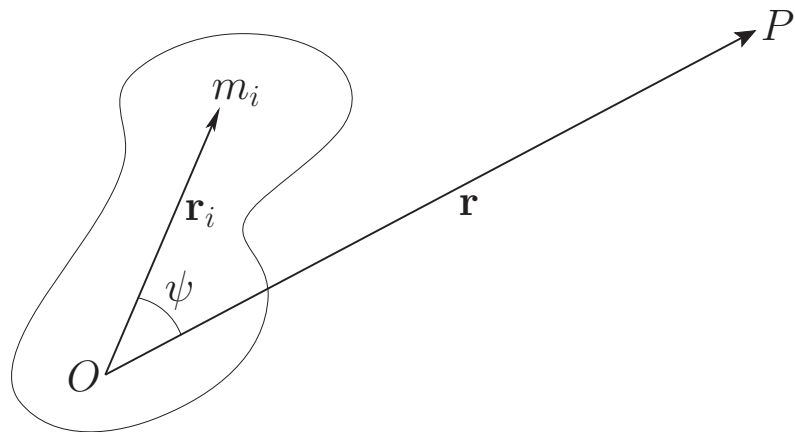


**Fig. 7.3** A general mass distribution.

Consider the gravitational potential,  $\Phi$ , generated by the mass distribution at some external point  $P$  whose position vector is  $\mathbf{r} \equiv (x, y, z)$ . According to Section 2.2,

$$\Phi(\mathbf{r}) = -G \sum_{i=1,N} \frac{m_i}{|\mathbf{r}_i - \mathbf{r}|}, \quad (7.74)$$

which can also be written

$$\Phi(\mathbf{r}) = -\frac{G}{r} \sum_{i=1,N} m_i \left( 1 - 2 \frac{r_i}{r} \cos \psi + \frac{r_i^2}{r^2} \right)^{-1/2}, \quad (7.75)$$

where  $\psi$  is the angle subtended between the vectors  $\mathbf{r}$  and  $\mathbf{r}_i$ . (See Figure 7.3.) Suppose that the distance  $OP \equiv r$  is much larger than the characteristic radius of the mass distribution, which implies that  $r_i/r \ll 1$  for all  $i$ . Expanding up to second order in  $r_i/r$ , we obtain

$$\Phi(\mathbf{r}) \approx -\frac{G}{r} \sum_{i=1,N} m_i \left[ 1 + \frac{r_i}{r} \cos \psi + \frac{1}{2} \frac{r_i^2}{r^2} (3 \cos^2 \psi - 1) \right]. \quad (7.76)$$

However,

$$\sum_{i=1,N} m_i \frac{r_i}{r} \cos \psi = \sum_{i=1,N} m_i \frac{\mathbf{r}_i \cdot \mathbf{r}}{r^2} = \sum_{i=1,N} m_i \frac{x_i x + y_i y + z_i z}{r^2} = 0, \quad (7.77)$$

where we have made use of Equation (7.69). Hence, we are left with

$$\Phi(\mathbf{r}) \approx -\frac{G M}{r} - \frac{G}{2r^3} \sum_{i=1,N} m_i r_i^2 (2 - 3 \sin^2 \psi). \quad (7.78)$$

Here,  $M = \sum_{i=1,N} m_i$  is the total mass of the distribution. Now,

$$\begin{aligned} \sum_{i=1,N} 2m_i r_i^2 &= \sum_{i=1,N} m_i (y_i^2 + z_i^2) + \sum_{i=1,N} m_i (x_i^2 + z_i^2) + \sum_{i=1,N} m_i (x_i^2 + y_i^2) \\ &= \mathcal{I}_{xx} + \mathcal{I}_{yy} + \mathcal{I}_{zz}, \end{aligned} \quad (7.79)$$

where we have made use of Equations (7.70)–(7.73). Furthermore,

$$\mathcal{I} \equiv \sum_{i=1,N} m_i r_i^2 \sin^2 \psi \quad (7.80)$$

is the distribution's moment of inertia about the axis  $OP$ . Thus, we deduce that

$$\Phi(\mathbf{r}) \simeq -\frac{G M}{r} - \frac{G (\mathcal{I}_{xx} + \mathcal{I}_{yy} + \mathcal{I}_{zz} - 3 \mathcal{I})}{2 r^3}. \quad (7.81)$$

This famous result is known as *MacCullagh's formula*, after its discoverer, the Irish mathematician James MacCullagh (1809–1847). Actually,

$$\begin{aligned} \sum_{i=1,N} m_i r_i^2 \sin^2 \psi &= \sum_{i=1,N} m_i \frac{(y_i^2 + z_i^2) x^2 + (x_i^2 + z_i^2) y^2 + (x_i^2 + y_i^2) z^2}{r^2} \\ &= \frac{\mathcal{I}_{xx} x^2 + \mathcal{I}_{yy} y^2 + \mathcal{I}_{zz} z^2}{r^2}. \end{aligned} \quad (7.82)$$

Hence, MacCullagh's formula can also be written in the alternative form

$$\Phi(\mathbf{r}) \simeq -\frac{G M}{r} - \frac{G (\mathcal{I}_{xx} + \mathcal{I}_{yy} + \mathcal{I}_{zz})}{2 r^3} + \frac{3 G (\mathcal{I}_{xx} x^2 + \mathcal{I}_{yy} y^2 + \mathcal{I}_{zz} z^2)}{2 r^5}. \quad (7.83)$$

Finally, for an axisymmetric distribution, such that  $\mathcal{I}_{xx} = \mathcal{I}_{yy} = \mathcal{I}_\perp$  and  $\mathcal{I}_{zz} = \mathcal{I}_\parallel$ , MacCullagh's formula reduces to

$$\Phi(\mathbf{r}) \simeq -\frac{G M}{r} + \frac{G (\mathcal{I}_\parallel - \mathcal{I}_\perp)}{r^3} P_2(\cos \theta), \quad (7.84)$$

where  $\cos \theta = z/r$ . Of course, this expression is the same as Equation (7.68), which justifies our earlier assertion that Equation (7.67) is valid for a general axisymmetric mass distribution. Incidentally, a comparison of the above expression with Equation (2.66) reveals that

$$J_2 = \frac{\mathcal{I}_\parallel - \mathcal{I}_\perp}{M R^2}, \quad (7.85)$$

where  $R$  is the mean radius of the distribution, and the dimensionless parameter  $J_2$  characterizes the quadrupole gravitational field external to the distribution.

## 7.10 Forced precession and nutation of the Earth

Consider the Earth–Sun system. (See Figure 7.4.) From a geocentric viewpoint, the Sun orbits the Earth counterclockwise (if we look from the north), once per year, in an approximately circular orbit of radius  $a_s = 1.50 \times 10^{11}$  m (Yoder 1995). In astronomy, the plane of the Sun's apparent orbit relative to the Earth is known as the *ecliptic plane*. Let us define *nonrotating* Cartesian coordinates, centered on the Earth, which are such that the  $x$ - and  $y$ -axes lie in the ecliptic plane, and the  $z$ -axis is normal to this plane (in the sense that the Earth's north pole lies at positive  $z$ ). It follows that the  $z$ -axis is directed toward a point in the sky (located in the constellation Draco) known as the *ecliptic north pole*. (See Figure 7.5.) In the following, we shall treat the  $x$ ,  $y$ ,  $z$  coordinate system as

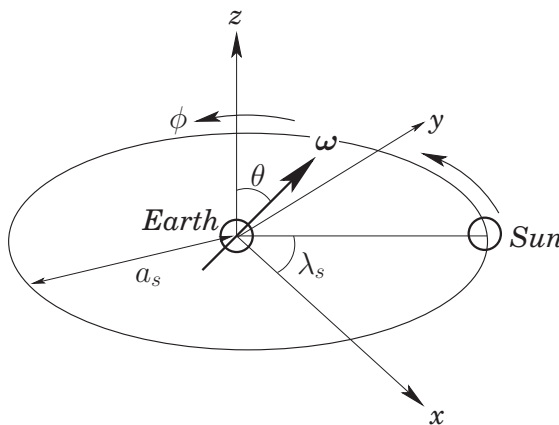


**Fig. 7.4** The Earth–Sun system.

inertial. This is a reasonable approximation because the orbital acceleration of the Earth is much smaller than the acceleration due to its diurnal rotation. It is convenient to parameterize the instantaneous position of the Sun in terms of a counterclockwise (if we look from the north) azimuthal angle  $\lambda_s$  that is zero on the positive  $x$ -axis. (See Figure 7.4.)

Let  $\omega$  be the Earth's angular velocity vector due to its daily rotation. This vector makes an angle  $\theta$  with the  $z$ -axis, where  $\theta = 23.44^\circ$  is the mean inclination of the ecliptic to the Earth's equatorial plane (Yoder 1995). Suppose that the projection of  $\omega$  onto the ecliptic plane subtends an angle  $\phi$  with the  $y$ -axis, where  $\phi$  is measured in a counterclockwise (if we look from the north) sense. (See Figure 7.4.) The orientation of the Earth's axis of rotation (which is, of course, parallel to  $\omega$ ) is thus determined by the two angles  $\theta$  and  $\phi$ . Note, however, that these two angles are also *Euler angles*, in the sense given in Section 7.7. Let us examine the Earth–Sun system at an instant in time,  $t = 0$ , when  $\phi = 0$ : that is, when  $\omega$  lies in the  $y-z$  plane. At this particular instant, the  $x$ -axis points toward the so-called vernal equinox, which is defined as the point in the sky where the Sun's apparent orbit crosses the projection of the Earth's equator (i.e., the plane normal to  $\omega$ ) from south to north. A counterclockwise (if we look from the north) angle in the ecliptic plane that is zero at the vernal equinox is generally known as an *ecliptic longitude*. Thus,  $\lambda_s$  is the Sun's ecliptic longitude.

According to Equation (7.68), the potential energy of the Earth–Sun system is written

$$U = M_s \Phi = -\frac{G M_s M}{a_s} + \frac{G M_s (\mathcal{I}_{\parallel} - \mathcal{I}_{\perp})}{a_s^3} P_2[\cos(\gamma_s)], \quad (7.86)$$

where  $M_s$  is the mass of the Sun,  $M$  the mass of the Earth,  $\mathcal{I}_{\parallel}$  the Earth's moment of inertia about its axis of rotation,  $\mathcal{I}_{\perp}$  the Earth's moment of inertia about an axis lying in its equatorial plane, and  $P_2(x) = (1/2)(3x^2 - 1)$ . Furthermore,  $\gamma_s$  is the angle subtended between  $\omega$  and  $\mathbf{r}_s$ , where  $\mathbf{r}_s$  is the position vector of the Sun relative to the Earth.

It is easily demonstrated that (with  $\phi = 0$ )

$$\omega = \omega(0, \sin \theta, \cos \theta) \quad (7.87)$$

and

$$\mathbf{r}_s = a_s (\cos \lambda_s, \sin \lambda_s, 0). \quad (7.88)$$

Hence,

$$\cos \gamma_s = \frac{\boldsymbol{\omega} \cdot \mathbf{r}_s}{|\boldsymbol{\omega}| |\mathbf{r}_s|} = \sin \theta \sin \lambda_s, \quad (7.89)$$

giving

$$U = -\frac{G M_s M}{a_s} + \frac{G M_s (\mathcal{I}_{\parallel} - \mathcal{I}_{\perp})}{2 a_s^3} (3 \sin^2 \theta \sin^2 \lambda_s - 1). \quad (7.90)$$

Given that we are primarily interested in the motion of the Earth's axis of rotation on timescales that are much longer than a year, we can average the preceding expression over the Sun's orbit to give

$$U = -\frac{G M_s M}{a_s} + \frac{G M_s (\mathcal{I}_{\parallel} - \mathcal{I}_{\perp})}{2 a_s^3} \left( \frac{3}{2} \sin^2 \theta - 1 \right) \quad (7.91)$$

(because the average of  $\sin^2 \lambda_s$  over a year is  $1/2$ ). Thus, we obtain

$$U = U_0 - \epsilon \alpha_s \cos(2\theta), \quad (7.92)$$

where  $U_0$  is a constant, and

$$\alpha_s = \frac{3}{8} \mathcal{I}_{\parallel} n_s^2. \quad (7.93)$$

Here,

$$\epsilon = \frac{\mathcal{I}_{\parallel} - \mathcal{I}_{\perp}}{\mathcal{I}_{\parallel}} = 0.00335 \quad (7.94)$$

is the Earth's ellipticity (Yoder 1995), and

$$n_s = \frac{d\lambda_s}{dt} = \left( \frac{G M_s}{a_s^3} \right)^{1/2} \quad (7.95)$$

is the Sun's apparent orbital angular velocity.

The rotational kinetic energy of the Earth can be written (see Section 7.4)

$$K = \frac{1}{2} (\mathcal{I}_{\perp} \omega_x^2 + \mathcal{I}_{\perp} \omega_y^2 + \mathcal{I}_{\parallel} \omega_z^2), \quad (7.96)$$

which reduces to

$$K = \frac{1}{2} (\mathcal{I}_{\perp} \dot{\theta}^2 + \mathcal{I}_{\perp} \sin^2 \theta \dot{\phi}^2 + \mathcal{I}_{\parallel} \omega^2) \quad (7.97)$$

with the aid of Equations (7.53)–(7.55). Here,

$$\omega = \cos \theta \dot{\phi} + \dot{\psi} \quad (7.98)$$

and  $\psi$  is the third Euler angle. Hence, the Earth's Lagrangian takes the form

$$\mathcal{L} = K - U = \frac{1}{2} (\mathcal{I}_{\perp} \dot{\theta}^2 + \mathcal{I}_{\perp} \sin^2 \theta \dot{\phi}^2 + \mathcal{I}_{\parallel} \omega^2) + \epsilon \alpha_s \cos(2\theta), \quad (7.99)$$

where any constant terms have been neglected. The Lagrangian does not depend explicitly on the angular coordinate  $\psi$ . It follows that the conjugate momentum is a constant of the motion (see Section 6.5). In other words,

$$p_\psi = \frac{\partial \mathcal{L}}{\partial \dot{\psi}} = \mathcal{I}_{\parallel} \omega \quad (7.100)$$

is a constant of the motion, implying that  $\omega$  is also a constant of the motion. Note that  $\omega$  is effectively the Earth's angular velocity of rotation about its axis [because  $|\omega_x|, |\omega_y| \ll \omega_z = \omega$ , which follows because  $|\dot{\phi}|, |\dot{\theta}| \ll \dot{\psi}$ ; see Equations (7.53)–(7.55)]. Another equation of motion that can be derived from the Lagrangian is

$$\frac{d}{dt} \left( \frac{\partial \mathcal{L}}{\partial \dot{\theta}} \right) - \frac{\partial \mathcal{L}}{\partial \theta} = 0, \quad (7.101)$$

which reduces to

$$\mathcal{I}_{\perp} \ddot{\theta} - \frac{\partial \mathcal{L}}{\partial \theta} = 0. \quad (7.102)$$

Consider *steady precession* of the Earth's rotational axis, which is characterized by  $\dot{\theta} = 0$ , with both  $\dot{\phi}$  and  $\dot{\psi}$  constant. It follows, from Equation (7.102), that such motion must satisfy the constraint

$$\frac{\partial \mathcal{L}}{\partial \theta} = 0. \quad (7.103)$$

Thus, we obtain

$$\frac{1}{2} \mathcal{I}_{\perp} \sin(2\theta) \dot{\phi}^2 - \mathcal{I}_{\parallel} \sin \theta \omega \dot{\phi} - 2\epsilon \alpha_s \sin(2\theta) = 0, \quad (7.104)$$

where we have made use of Equations (7.98) and (7.99). As we can easily verify after the fact,  $|\dot{\phi}| \ll \omega$ , so Equation (7.104) reduces to

$$\dot{\phi} \simeq -\frac{4\epsilon \alpha_s \cos \theta}{\mathcal{I}_{\parallel} \omega} = \Omega_\phi, \quad (7.105)$$

which can be integrated to give

$$\phi \simeq -\Omega_\phi t, \quad (7.106)$$

where

$$\Omega_\phi = \frac{3}{2} \frac{\epsilon n_s^2}{\omega} \cos \theta \quad (7.107)$$

and we have made use of Equation (7.93). According to the preceding expressions, the mutual interaction between the Sun and the quadrupole gravitational field generated by the Earth's slight oblateness causes the Earth's axis of rotation to precess steadily about the normal to the ecliptic plane at the rate  $-\Omega_\phi$ . The fact that  $-\Omega_\phi$  is negative implies that the precession is in the *opposite* sense to that of the Earth's diurnal rotation and the Sun's apparent orbit about the Earth. Incidentally, the interaction causes a precession of the Earth's rotational axis, rather than the plane of the Sun's orbit, because the Earth's axial moment of inertia is much less than the Sun's orbital moment of inertia. The precession period in (sidereal) years is given by

$$T_\phi(\text{yr}) = \frac{n_s}{\Omega_\phi} = \frac{2 T_s(\text{day})}{3\epsilon \cos \theta}, \quad (7.108)$$

where  $T_s(\text{day}) = \omega/n_s = 365.26$  is the length of a sidereal year in days. Thus, given that  $\epsilon = 0.00335$  and  $\theta = 23.44^\circ$ , we obtain

$$T_\phi \simeq 79,200 \text{ years.} \quad (7.109)$$

Unfortunately, the observed precession period of the Earth's axis of rotation about the normal to the ecliptic plane is approximately 25,800 years (Yoder 1995), so something is clearly missing from our model. It turns out that the missing factor is the influence of the *Moon*.

Using analogous arguments to those given previously, we can write the potential energy of the Earth–Moon system can be written

$$U = -\frac{G M_m M}{a_m} + \frac{G M_m (\mathcal{I}_{\parallel} - \mathcal{I}_{\perp})}{a_m^3} P_2[\cos(\gamma_m)], \quad (7.110)$$

where  $M_m$  is the lunar mass, and  $a_m$  the radius of the Moon's (approximately circular) orbit. Furthermore,  $\gamma_m$  is the angle subtended between  $\boldsymbol{\omega}$  and  $\mathbf{r}_m$ , where

$$\boldsymbol{\omega} = \omega (-\sin \theta \sin \phi, \sin \theta \cos \phi, \cos \theta) \quad (7.111)$$

is the Earth's angular velocity vector and  $\mathbf{r}_m$  is the position vector of the Moon relative to the Earth. Here, for the moment, we have retained the  $\phi$  dependence in our expression for  $\boldsymbol{\omega}$  (because we shall presently differentiate by  $t$  before setting  $\phi = 0$ ). The Moon's orbital plane is actually slightly inclined to the ecliptic plane, the (mean) angle of inclination being  $I_m = 5.16^\circ$  (Yoder 1995). Hence, we can write

$$\mathbf{r}_m \simeq a_m (\cos \lambda_m, \sin \lambda_m, I_m \sin(\lambda_m - \alpha_n)), \quad (7.112)$$

to first order in  $I_m$ , where  $\lambda_m$  is the Moon's ecliptic longitude and  $\alpha_n$  is the ecliptic longitude of the lunar *ascending node*, which is defined as the point on the lunar orbit where the Moon crosses the ecliptic plane from south to north. Of course,  $\lambda_m$  increases at the rate  $n_m$ , where

$$n_m = \frac{d\lambda_m}{dt} \simeq \left( \frac{GM}{a_m^3} \right)^{1/2} \quad (7.113)$$

is the Moon's mean orbital angular velocity. It turns out that the lunar ascending node precesses steadily, in the opposite direction to the Moon's orbital rotation, in such a manner that it completes a full circuit every 18.6 years (Yoder 1995). This precession is caused by the perturbing influence of the Sun. (See Chapter 10.) It follows that

$$\frac{d\alpha_n}{dt} = -\mathcal{Q}_n, \quad (7.114)$$

where  $2\pi/\mathcal{Q}_n = 18.6$  years. From Equations (7.111) and (7.112),

$$\cos \gamma_m = \frac{\boldsymbol{\omega} \cdot \mathbf{r}_m}{|\boldsymbol{\omega}| |\mathbf{r}_m|} = \sin \theta \sin(\lambda_m - \phi) + I_m \cos \theta \sin(\lambda_m - \alpha_n), \quad (7.115)$$

so Equation (7.110) yields

$$\begin{aligned} U \simeq & -\frac{G M_m M}{a_m} + \frac{G M_m (\mathcal{I}_{\parallel} - \mathcal{I}_{\perp})}{2 a_m^3} [3 \sin^2 \theta \sin^2(\lambda_m - \phi) \\ & + 3 I_m \sin(2\theta) \sin(\lambda_m - \phi) \sin(\lambda_m - \alpha_n) - 1] \end{aligned} \quad (7.116)$$

to first order in  $I_m$ . Given that we are interested in the motion of the Earth's axis of rotation on timescales that are much longer than a month, we can average this expression over the Moon's orbit to give

$$U \simeq U'_0 - \epsilon \alpha_m \cos(2\theta) + \epsilon \beta_m \sin(2\theta) \cos(\alpha_n - \phi), \quad (7.117)$$

[because the average of  $\sin^2(\lambda_m - \phi)$  over a month is 1/2, whereas that of  $\sin(\lambda_m - \phi) \sin(\lambda_m - \alpha_n)$  is  $(1/2) \cos(\alpha_n - \phi)$ ]. Here,  $U'_0$  is a constant,

$$\alpha_m = \frac{3}{8} \mathcal{I}_{\parallel} \mu_m n_m^2, \quad (7.118)$$

$$\beta_m = \frac{3}{4} \mathcal{I}_{\parallel} I_m \mu_m n_m^2, \quad (7.119)$$

and

$$\mu_m = \frac{M_m}{M} = 0.0123 \quad (7.120)$$

is the ratio of the lunar to the terrestrial mass (Yoder 1995). Gravity is a superposable force, so the total potential energy of the Earth–Moon–Sun system is the sum of Equations (7.92) and (7.117). In other words,

$$U = U''_0 - \epsilon \alpha \cos(2\theta) + \epsilon \beta_m \sin(2\theta) \cos(\alpha_n - \phi), \quad (7.121)$$

where  $U''_0$  is a constant and

$$\alpha = \alpha_s + \alpha_m. \quad (7.122)$$

Finally, making use of Equation (7.97), the Lagrangian of the Earth is written

$$\mathcal{L} = \frac{1}{2} \left( \mathcal{I}_{\perp} \dot{\theta}^2 + \mathcal{I}_{\perp} \sin^2 \theta \dot{\phi}^2 + \mathcal{I}_{\parallel} \omega^2 \right) + \epsilon \alpha \cos(2\theta) - \epsilon \beta_m \sin(2\theta) \cos(\alpha_n - \phi), \quad (7.123)$$

where any constant terms have been neglected. Recall that  $\omega$  is given by Equation (7.98) and is a constant of the motion.

Two equations of motion that can immediately be derived from the preceding Lagrangian are

$$\frac{d}{dt} \left( \frac{\partial \mathcal{L}}{\partial \dot{\theta}} \right) - \frac{\partial \mathcal{L}}{\partial \theta} = 0 \quad (7.124)$$

and

$$\frac{d}{dt} \left( \frac{\partial \mathcal{L}}{\partial \dot{\phi}} \right) - \frac{\partial \mathcal{L}}{\partial \phi} = 0. \quad (7.125)$$

(The third equation, involving  $\psi$ , merely confirms that  $\omega$  is a constant of the motion.) These above two equations yield

$$\begin{aligned} 0 &= \mathcal{I}_{\perp} \ddot{\theta} - \frac{1}{2} \mathcal{I}_{\perp} \sin(2\theta) \dot{\phi}^2 + \mathcal{I}_{\parallel} \sin \theta \omega \dot{\phi} + 2\epsilon \alpha \sin(2\theta) \\ &\quad + 2\epsilon \beta_m \cos(2\theta) \cos(\alpha_n - \phi), \end{aligned} \quad (7.126)$$

and

$$0 = \frac{d}{dt} \left( \mathcal{I}_{\perp} \sin^2 \theta \dot{\phi} + \mathcal{I}_{\parallel} \cos \theta \omega \right) + \epsilon \beta_m \sin(2\theta) \sin(\alpha_n - \phi), \quad (7.127)$$

respectively. Let

$$\theta(t) = \theta_0 + \epsilon \theta_1(t), \quad (7.128)$$

and

$$\phi(t) = \epsilon \phi_1(t), \quad (7.129)$$

where  $\theta_0 = 23.44^\circ$  is the mean inclination of the ecliptic to the Earth's equatorial plane. To first order in  $\epsilon$ , Equations (7.126) and (7.127) reduce to

$$0 \simeq \mathcal{I}_\perp \ddot{\theta}_1 + \mathcal{I}_\parallel \sin \theta_0 \omega \dot{\phi}_1 + 2\alpha \sin(2\theta_0) + 2\beta_m \cos(2\theta_0) \cos(\Omega_n t) \quad (7.130)$$

and

$$0 \simeq \mathcal{I}_\perp \sin^2 \theta_0 \ddot{\phi}_1 - \mathcal{I}_\parallel \sin \theta_0 \omega \dot{\theta}_1 - \beta_m \sin(2\theta_0) \sin(\Omega_n t), \quad (7.131)$$

respectively, where use has been made of Equation (7.114). However, as can easily be verified after the fact,  $d/dt \ll \omega$ , so we obtain

$$\dot{\phi}_1 \simeq -\frac{4\alpha \cos \theta_0}{\mathcal{I}_\parallel \omega} - \frac{2\beta_m \cos(2\theta_0)}{\mathcal{I}_\parallel \omega \sin \theta_0} \cos(\Omega_n t) \quad (7.132)$$

and

$$\dot{\theta}_1 \simeq -\frac{2\beta_m \cos \theta_0}{\mathcal{I}_\parallel \omega} \sin(\Omega_n t). \quad (7.133)$$

These equations can be integrated and then combined with Equations (7.128) and (7.129) to give

$$\phi(t) = -\Omega_\phi t - \delta\phi \sin(\Omega_n t) \quad (7.134)$$

and

$$\theta(t) = \theta_0 + \delta\theta \cos(\Omega_n t), \quad (7.135)$$

where

$$\Omega_\phi = \frac{3}{2} \frac{\epsilon(n_s^2 + \mu_m n_m^2)}{\omega} \cos \theta_0, \quad (7.136)$$

$$\delta\phi = \frac{3}{2} \frac{\epsilon I_m \mu_m n_m^2}{\omega \Omega_n} \frac{\cos(2\theta_0)}{\sin \theta_0}, \quad (7.137)$$

and

$$\delta\theta = \frac{3}{2} \frac{\epsilon I_m \mu_m n_m^2}{\omega \Omega_n} \cos \theta_0. \quad (7.138)$$

Incidentally, in these expressions, we have assumed that the lunar ascending node coincides with the vernal equinox at time  $t = 0$  (i.e.,  $\alpha_n = 0$  at  $t = 0$ ), in accordance with our previous assumption that  $\phi = 0$  at  $t = 0$ .

According to Equation (7.134), the combined gravitational interaction of the Sun and the Moon with the gravitational quadrupole field generated by the Earth's slight oblateness causes the Earth's axis of rotation to precess steadily about the normal to the ecliptic plane at the rate  $-\Omega_\phi$ . As before, the negative sign indicates that the precession

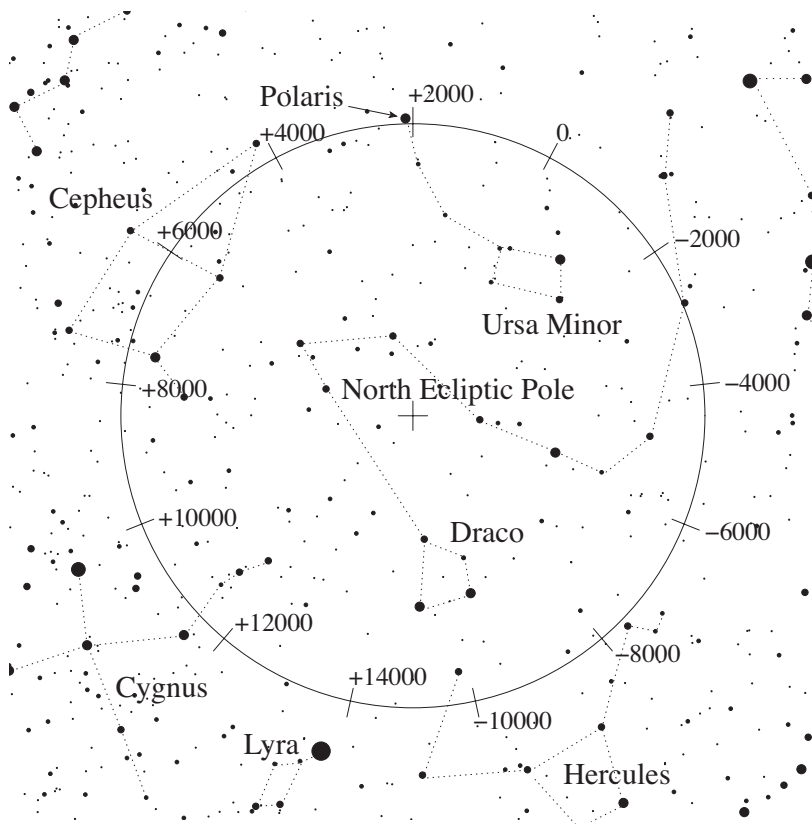


**Fig. 7.5** Path of the north celestial pole against the backdrop of the stars as consequence of the precession of the equinoxes (calculated assuming constant precessional speed and obliquity). Numbers indicate years relative to the start of the common era. Stellar positions and magnitudes from Hoffleit and Warren 1991.

is in the opposite direction to the (apparent) orbital motion of the Sun and the Moon. The period of this so-called *luni-solar precession* in (sidereal) years is given by

$$T_\phi(\text{yr}) = \frac{n_s}{\Omega_\phi} = \frac{2 T_s(\text{day})}{3 \epsilon \{1 + \mu_m/[T_m(\text{yr})]^2\} \cos \theta_0}, \quad (7.139)$$

where  $T_m(\text{yr}) = n_s/n_m = 0.081$  is the Moon's (synodic) orbital period in years. Given that  $\epsilon = 0.00335$ ,  $\theta_0 = 23.44^\circ$ ,  $T_s(\text{day}) = 365.26$ , and  $\mu_m = 0.0123$ , we obtain

$$T_\phi \approx 27,600 \text{ years.} \quad (7.140)$$

This prediction is fairly close to the observed precession period of 25,800 years (Yoder 1995). The main reason that our estimate is slightly inaccurate is because we have neglected to take into account the small eccentricities of the Earth's orbit around the Sun and the Moon's orbit around the Earth.

The point in the sky toward which the Earth's axis of rotation points is known as the *north celestial pole*. Currently, this point lies within about a degree of the fairly bright star Polaris, which is consequently sometimes known as the *north star* or *pole star*. (See Figure 7.5.) It follows that Polaris appears to be almost stationary in the sky, always

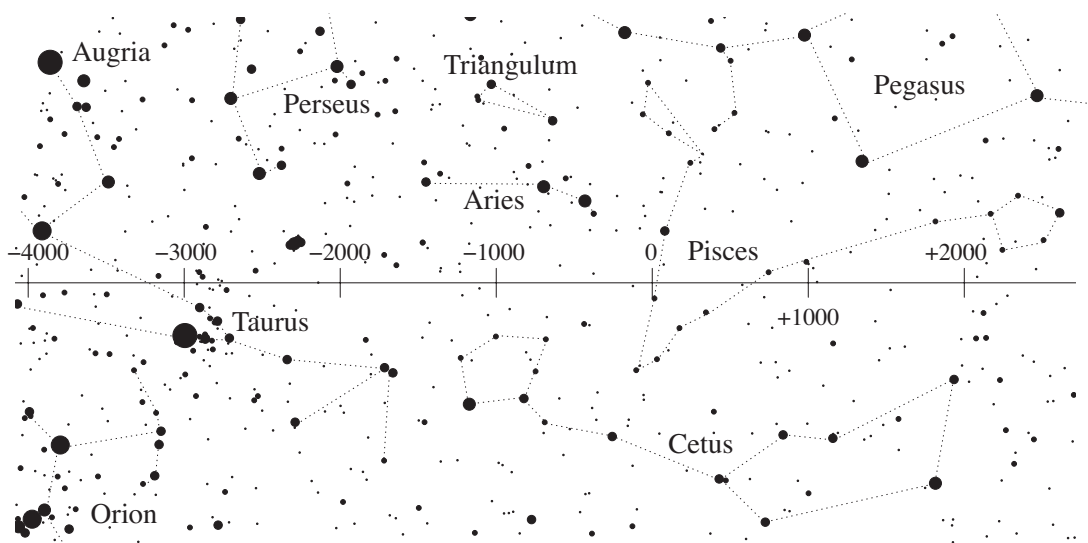


**Fig. 7.6** Path of the vernal equinox against the backdrop of the stars as a consequence of the precession of the equinoxes (calculated assuming constant precessional speed and obliquity). Numbers indicate years relative to the start of the common era. Stellar positions and magnitudes from Hoffleit and Warren 1991.

lying due north, and can thus be used for navigational purposes. Indeed, mariners have relied on the north star for many hundreds of years to determine direction at sea. Unfortunately, because of the precession of the Earth's axis of rotation, the north celestial pole is not a fixed point in the sky but instead traces out a circle, of angular radius  $23.44^\circ$ , about the north ecliptic pole, with a period of 25,800 years. (See Figure 7.5.) Hence, a few thousand years from now, the north celestial pole will no longer coincide with Polaris, and there will be no convenient way of telling direction from the stars.

The projection of the ecliptic plane onto the sky is called the *ecliptic circle* and coincides with the apparent path of the Sun against the backdrop of the stars. The projection of the Earth's equator onto the sky is known as the *celestial equator*. As has been previously mentioned, the ecliptic is inclined at  $23.44^\circ$  to the celestial equator. The two points in the sky at which the ecliptic crosses the celestial equator are called the *equinoxes*, as night and day are equally long when the Sun lies at these points. Thus, the Sun reaches the vernal equinox on about March 20, and this traditionally marks the beginning of spring. Likewise, the Sun reaches the autumnal equinox on about September 22, and this traditionally marks the beginning of autumn. However, the precession of the Earth's axis of rotation causes the celestial equator (which is always normal to this axis) to precess in the sky; it thus also causes the equinoxes to precess along the ecliptic. This effect is known as the *precession of the equinoxes*. The precession is in the opposite direction to the Sun's apparent motion around the ecliptic and is of magnitude  $1.4^\circ$  per century. Amazingly, this minuscule effect was discovered by the ancient Greeks (with the help of ancient Babylonian observations; Heath 1991). In about 2000 BCE, when the science of astronomy originated in ancient Egypt and Babylonia, the vernal equinox lay in the constellation Aries. (See Figure 7.6.) Indeed, the vernal equinox is

still sometimes called the *first point of Aries* in astronomical texts. About 90 BCE, the vernal equinox moved into the constellation Pisces, where it still remains. The equinox will move into the constellation Aquarius (marking the beginning of the much-heralded “Age of Aquarius”) in about 2600 CE. Incidentally, the position of the vernal equinox in the sky is of great significance in astronomy, as it is used as the zero of celestial longitude (much as the Greenwich meridian is used as the zero of terrestrial longitude).

Equations (7.134) and (7.135) indicate that the small inclination of the lunar orbit to the ecliptic plane, combined with the precession of the lunar ascending node, causes the Earth’s axis of rotation to wobble slightly. This wobble is known as *nutation* (from the Latin *nutare*, to nod) and is superimposed on the aforementioned precession. In the absence of precession, nutation would cause the north celestial pole to periodically trace out a small ellipse on the sky, the sense of rotation being counterclockwise. The nutation period is 18.6 years—the same as the precession period of the lunar ascending node. The nutation amplitudes in the polar and azimuthal angles  $\theta$  and  $\phi$  are

$$\delta\theta = \frac{3}{2} \frac{\epsilon I_m \mu_m T_n(\text{yr})}{T_s(\text{day}) [T_m(\text{yr})]^2} \cos \theta_0 \quad (7.141)$$

and

$$\delta\phi = \frac{3}{2} \frac{\epsilon I_m \mu_m T_n(\text{yr})}{T_s(\text{day}) [T_m(\text{yr})]^2} \frac{\cos(2\theta_0)}{\sin \theta_0}, \quad (7.142)$$

respectively, where  $T_n(\text{yr}) = n_s/\Omega_n = 18.6$ . Given that  $\epsilon = 0.00335$ ,  $\theta_0 = 23.44^\circ$ ,  $I_m = 5.16^\circ$ ,  $T_s(\text{day}) = 365.26$ ,  $T_m(\text{yr}) = 0.081$ , and  $\mu_m = 0.0123$ , we obtain

$$\delta\theta = 8.2'' \quad (7.143)$$

and

$$\delta\phi = 15.3''. \quad (7.144)$$

The observed nutation amplitudes are  $9.2''$  and  $17.2''$ , respectively (Meeus 2005). Hence, our estimates are quite close to the mark. Any inaccuracy is mainly due to the fact that we have neglected to take into account the small eccentricities of the Earth’s orbit around the Sun and the Moon’s orbit around the Earth. The nutation of the Earth was discovered in 1728 by the English astronomer James Bradley (1693–1748); it was explained theoretically about 20 years later by d’Alembert and Euler. Nutation is important because the corresponding gyration of the Earth’s rotation axis appears to be transferred to celestial objects when they are viewed using terrestrial telescopes. This effect causes the celestial longitudes and latitudes of heavenly objects to oscillate sinusoidally by up to  $20''$  (i.e., about the maximum apparent angular size of Saturn) with a period of 18.6 years. It is necessary to correct for this oscillation (as well as for the precession of the equinoxes) to accurately guide terrestrial telescopes to particular celestial objects.

## 7.11 Spin-orbit coupling

Let us investigate the spinning motion (i.e., the rotational motion about an axis passing through the center of mass) of an *aspherical* moon in a Keplerian elliptical orbit about

a spherically symmetric planet of mass  $m_p$ . It is convenient to analyze this motion in a frame of reference whose origin always coincides with the moon's center of mass,  $O$ . Let us define a Cartesian coordinate system  $x, y, z$  whose axes are aligned with the moon's principal axes of rotation, and let  $\mathcal{I}_{xx}, \mathcal{I}_{yy}, \mathcal{I}_{zz}$  be the corresponding principal moments of inertia. Suppose that  $\mathcal{I}_{zz} > \mathcal{I}_{yy} > \mathcal{I}_{xx}$ , which implies that the moon's radius attains its greatest and least values at those points where the  $x$ - and  $z$ -axes pierce its surface, respectively (assuming that the moon's shape is roughly ellipsoidal). Let the planet,  $P$ , be located at position vector  $\mathbf{r} \equiv (x, y, z)$ . We can treat the planet as a point mass, as it is spherically symmetric. Incidentally, we are assuming that the moon's deviations from spherical symmetry are of a permanent nature, being maintained by internal tensile strength rather than being induced by tidal or rotational effects.

According to MacCullagh's formula, the gravitational potential produced at  $P$  by the gravitational field of the moon is (see Section 7.9)

$$\Phi(\mathbf{r}) \approx -\frac{G M}{r} - \frac{G (\mathcal{I}_{xx} + \mathcal{I}_{yy} + \mathcal{I}_{zz})}{2 r^3} + \frac{3 G (\mathcal{I}_{xx} x^2 + \mathcal{I}_{yy} y^2 + \mathcal{I}_{zz} z^2)}{2 r^5}. \quad (7.145)$$

Thus, the gravitational force,  $\mathbf{f}$ , exerted on the planet by the moon has the components

$$f_x = -m_p \frac{\partial \Phi}{\partial x}, \quad (7.146)$$

$$f_y = -m_p \frac{\partial \Phi}{\partial y}, \quad (7.147)$$

and

$$f_z = -m_p \frac{\partial \Phi}{\partial z}. \quad (7.148)$$

Furthermore, the components of the torque,  $\boldsymbol{\tau}$ , acting on the planet about point  $O$  are

$$\tau_x = y f_z - z f_y = -\frac{3 G m_p (\mathcal{I}_{zz} - \mathcal{I}_{yy}) z y}{r^5}, \quad (7.149)$$

$$\tau_y = z f_x - x f_z = -\frac{3 G m_p (\mathcal{I}_{xx} - \mathcal{I}_{zz}) x z}{r^5}, \quad (7.150)$$

and

$$\tau_z = x f_y - y f_x = -\frac{3 G m_p (\mathcal{I}_{yy} - \mathcal{I}_{xx}) y x}{r^5}. \quad (7.151)$$

Of course, an equal and opposite torque,  $-\boldsymbol{\tau}$ , acts on the moon.

Euler's equations for the moon's spinning motion take the form (see Section 7.6)

$$\mathcal{I}_{xx} \dot{\omega}_x - (\mathcal{I}_{yy} - \mathcal{I}_{zz}) \omega_z \omega_y = -\tau_x, \quad (7.152)$$

$$\mathcal{I}_{yy} \dot{\omega}_y - (\mathcal{I}_{zz} - \mathcal{I}_{xx}) \omega_x \omega_z = -\tau_y, \quad (7.153)$$

and

$$\mathcal{I}_{zz} \dot{\omega}_z - (\mathcal{I}_{xx} - \mathcal{I}_{yy}) \omega_y \omega_x = -\tau_z, \quad (7.154)$$

where  $\boldsymbol{\omega} \equiv (\omega_x, \omega_y, \omega_z)$  is the associated angular velocity vector. Suppose that the moon is actually spinning about the  $z$ -axis (i.e., the principal axis of rotation with the largest

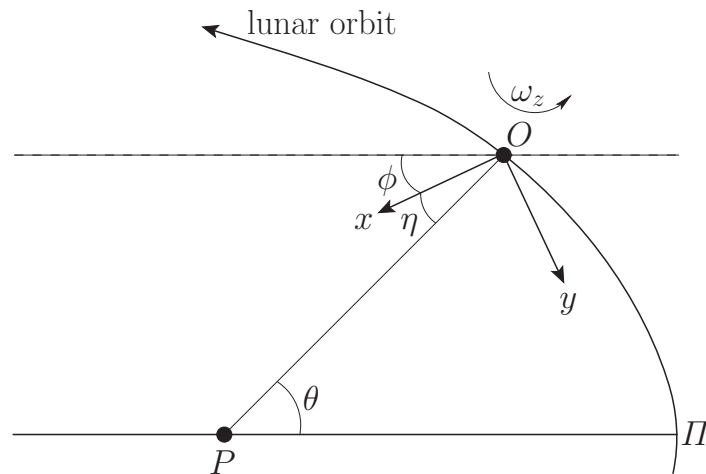


**Fig. 7.7** Geometry of spin-orbit coupling.

associated moment of inertia), and that this axis is directed *normal* to the moon's orbital plane (which is assumed to be fixed). It follows that

$$\omega = (0, 0, \omega_z) \quad (7.155)$$

and

$$\mathbf{r} = r (\cos \eta, \sin \eta, 0), \quad (7.156)$$

where  $\eta$  is the relative position angle of the planet in the  $x$ - $y$  plane. (See Figure 7.7.) We can write  $\omega_z = \dot{\phi}$ , where  $\phi$  is the angle subtended between the  $x$ -axis (say) and some fixed (with respect to distant stars) direction in the  $x$ - $y$  plane. Let this direction be parallel to the major axis  $P\Pi$  of the moon's orbit, where  $\Pi$  is the *pericenter* (i.e., the point of closest approach of the moon to the planet). In this case, it is clear from Figure 7.7 that

$$\eta = \theta - \phi, \quad (7.157)$$

where  $\theta$  is the moon's orbital true anomaly. (See Chapter 3.) Hence, Equations (7.151), (7.154), (7.155), and (7.156) yield

$$\ddot{\phi} + \frac{3}{2} n^2 \left( \frac{\mathcal{I}_{yy} - \mathcal{I}_{xx}}{\mathcal{I}_{zz}} \right) \left( \frac{a}{r} \right)^3 \sin[2(\phi - \theta)] = 0, \quad (7.158)$$

where use has been made of the standard Keplerian result  $G m_p = n^2 a^3$  (assuming that the mass of the moon is much less than that of the planet). (See Chapter 3.) Here,  $a$  and  $n$  are the moon's orbital major radius and mean angular velocity, respectively.

Assuming that the eccentricity,  $e$ , of the moon's orbit is low—so that  $0 \leq e \ll 1$ —it follows from Equations (3.85) and (3.86), as well as the trigonometric inequalities listed

in Section A.3, that

$$\left(\frac{a}{r}\right)^3 = 1 + 3e \cos \mathcal{M} + \mathcal{O}(e^2), \quad (7.159)$$

$$\theta = \mathcal{M} + 2e \sin \mathcal{M} + \mathcal{O}(e^2), \quad (7.160)$$

$$\cos 2\theta = \cos 2\mathcal{M} + 2e(\cos 3\mathcal{M} - \cos \mathcal{M}) + \mathcal{O}(e^2), \quad (7.161)$$

and

$$\sin 2\theta = \sin 2\mathcal{M} + 2e(\sin 3\mathcal{M} - \sin \mathcal{M}) + \mathcal{O}(e^2), \quad (7.162)$$

where  $\mathcal{M}$  is the moon's mean anomaly. Note that  $d\mathcal{M}/dt = n$ . Hence, Equation (7.158) gives

$$\begin{aligned} \ddot{\phi} \simeq & -\frac{3}{2} n^2 \left( \frac{\mathcal{I}_{yy} - \mathcal{I}_{xx}}{\mathcal{I}_{zz}} \right) \left[ -\frac{e}{2} \sin(2\phi - \mathcal{M}) + \sin(2\phi - 2\mathcal{M}) \right. \\ & \left. + \frac{7e}{2} \sin(2\phi - 3\mathcal{M}) \right], \end{aligned} \quad (7.163)$$

where any  $\mathcal{O}(e^2)$  terms have been neglected. Here, use has again been made of the trigonometric identities in Section A.3.

Suppose that the moon passes through its pericenter at time  $t = 0$ , so that

$$\mathcal{M} = nt. \quad (7.164)$$

In this case, the previous equation becomes

$$\frac{d^2\phi}{dt^2} \simeq -\frac{n_0^2}{2} \left[ -\frac{e}{2} \sin(2\phi - nt) + \sin(2\phi - 2nt) + \frac{7e}{2} \sin(2\phi - 3nt) \right], \quad (7.165)$$

where the so-called *asphericity parameter*,

$$\alpha = \left[ 3 \left( \frac{\mathcal{I}_{yy} - \mathcal{I}_{xx}}{\mathcal{I}_{zz}} \right) \right]^{1/2}, \quad (7.166)$$

is a measure of the moon's departure from spherical symmetry, and

$$n_0 = \alpha n. \quad (7.167)$$

Equation (7.165) is highly nonlinear in nature. Consequently, it does not possess a general analytic solution. Fortunately, Equation (7.165) is relatively straightforward to solve numerically. In fact, the solution can be represented as a trajectory in  $\phi, n^{-1} d\phi/dt, nt$  space. Because Equation (7.165) is deterministic, a trajectory that corresponds to a unique set of initial conditions cannot intersect a second trajectory that corresponds to a different set of initial conditions. Unfortunately, it is difficult to visualize a trajectory in three dimensions. However, we can alleviate this problem by plotting only those points where the trajectory pierces a set of equally spaced planes normal to the  $nt$  axis. These planes are located at  $nt = i2\pi$ , where  $i$  is an integer. This procedure is equivalent to projecting the trajectory onto the  $\phi, n^{-1} d\phi/dt$  plane each time the moon passes through its pericenter. The resulting plot is known as a *surface of section*. Figure 7.8 shows the surface of section for a set of trajectories corresponding to many different initial conditions. All of the trajectories are calculated from Equation (7.165) using  $\alpha = 0.15$

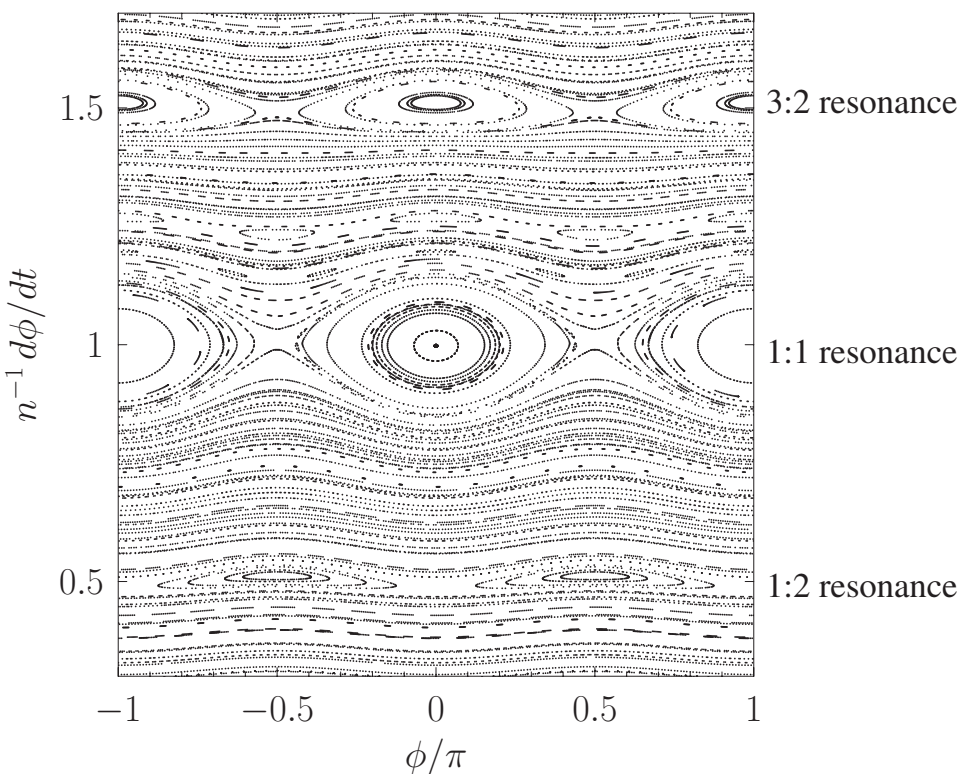


**Fig. 7.8** Surface of section plot for solutions of Equation (7.165) with  $\alpha = 0.15$  and  $e = 0.05$ . The major spin-orbit resonances are labeled.

and  $e = 0.05$ . The relatively small value adopted for the eccentricity,  $e$ , is consistent with our earlier assumption that the moon's orbit is nearly circular. On the other hand, the relatively small value adopted for the asphericity parameter,  $\alpha$ , implies that the moon is almost spherical. It can be seen, from Figure 7.8, that a trajectory corresponding to a given set of initial conditions generates a series of closely spaced points that trace out a closed curve running roughly parallel to the  $\phi$ -axis. Actually, there are two distinct types of curve. The majority of curves extend over all values of  $\phi$  and represent trajectories for which there is no particular correlation between the moon's spin and orbital motions. However, a relatively small number of curves extend over only a limited range of  $\phi$  values. These curves represent trajectories for which a *resonant interaction* between the moon's spin and orbital motions produces a strong correlation between these two types of motion. The exact resonances correspond to the centers of the eye-shaped structures that can be seen in Figure 7.8. The three principal spin-orbit resonances evident in the figure are the 1:2, 1:1, and 3:2 resonances. Here, a  $j_o:j_s$  resonance, where  $j_o$  and  $j_s$  are positive integers, is such that  $j_o$  times the moon's spin period is equal to  $j_s$  times its orbital period. At such a resonance, the moon's principal axes of rotation point in the *same* direction every  $j_s$  pericenter passages.

Consider the  $j_o:j_s$  spin-orbit resonance. It is helpful to define

$$\gamma = \phi - p \mathcal{M} = \phi - p n t, \quad (7.168)$$

where  $p = j_o/j_s$ . Here,  $\gamma$  is minus the angle subtended between the moon's  $x$ -axis and the major axis of its orbit every  $j_s$  passages through the pericenter. Note that  $\gamma = \phi$  at such passages. In the vicinity of the resonance, we expect  $\gamma$  to be a relatively slowly varying function of time. When expressed in terms of  $\gamma$ , Equation (7.165) yields

$$\begin{aligned} \frac{d^2\gamma}{dt^2} \simeq & -\frac{n_0^2}{2} \left( \left\{ -\frac{e}{2} \cos[(2p-1)nt] + \cos[2(p-1)nt] + \frac{7e}{2} \cos[(2p-3)nt] \right\} \sin 2\gamma \right. \\ & \left. + \left\{ -\frac{e}{2} \sin[(2p-1)nt] + \sin[2(p-1)nt] + \frac{7e}{2} \sin[(2p-3)nt] \right\} \cos 2\gamma \right). \end{aligned} \quad (7.169)$$

Let us now average the right-hand side of the above equation over  $j_s$  orbital periods, treating the relatively slowly varying quantity  $\gamma$  as a constant. For the 1:1 resonance, for which  $p = 1$ , we are left with

$$\frac{d^2\gamma}{dt^2} \simeq -\frac{1}{2} n_0^2 \sin 2\gamma. \quad (7.170)$$

This follows because  $\langle \cos[2(p-1)nt] \rangle = \langle 1 \rangle = 1$ , when  $p = 1$ , whereas all the other averages over rapidly varying terms are zero: e.g.,  $\langle \cos[(2p-1)nt] \rangle = \langle \cos(nt) \rangle = 0$ . For the 1:2 resonance, for which  $p = 1/2$ , we are left with

$$\frac{d^2\gamma}{dt^2} \simeq \frac{e}{4} n_0^2 \sin 2\gamma. \quad (7.171)$$

Finally, for the 3:2 resonance, for which  $p = 3/2$ , we are left with

$$\frac{d^2\gamma}{dt^2} \simeq -\frac{7e}{2} n_0^2 \sin 2\gamma. \quad (7.172)$$

Consider the 1:1 resonance. Multiplying Equation (7.170) by  $d\gamma/dt$ , and integrating, we obtain

$$\frac{1}{2} \left( \frac{d\gamma}{dt} \right)^2 - \frac{1}{4} n_0^2 \cos 2\gamma \simeq \frac{1}{4} n_0^2 \mathcal{E}, \quad (7.173)$$

where the constant  $\mathcal{E}$  is related to the moon's spin energy per unit mass. Now,  $n^{-1} d\gamma/dt = n^{-1} d\phi/dt - 1$ . Furthermore,  $\phi = \gamma$  at the times of pericenter passage. Hence, at such times,

$$\mathcal{E} \simeq \frac{2}{a^2} \left( n^{-1} \frac{d\phi}{dt} - 1 \right)^2 - \cos 2\phi. \quad (7.174)$$

Similar arguments reveal that

$$\mathcal{E} \simeq \frac{4}{e \alpha^2} \left( n^{-1} \frac{d\phi}{dt} - \frac{1}{2} \right)^2 + \cos 2\phi \quad (7.175)$$

for the 1:2 resonance and

$$\mathcal{E} \simeq \frac{4}{7e \alpha^2} \left( n^{-1} \frac{d\phi}{dt} - \frac{3}{2} \right)^2 - \cos 2\phi \quad (7.176)$$

for the 3:2 resonance.

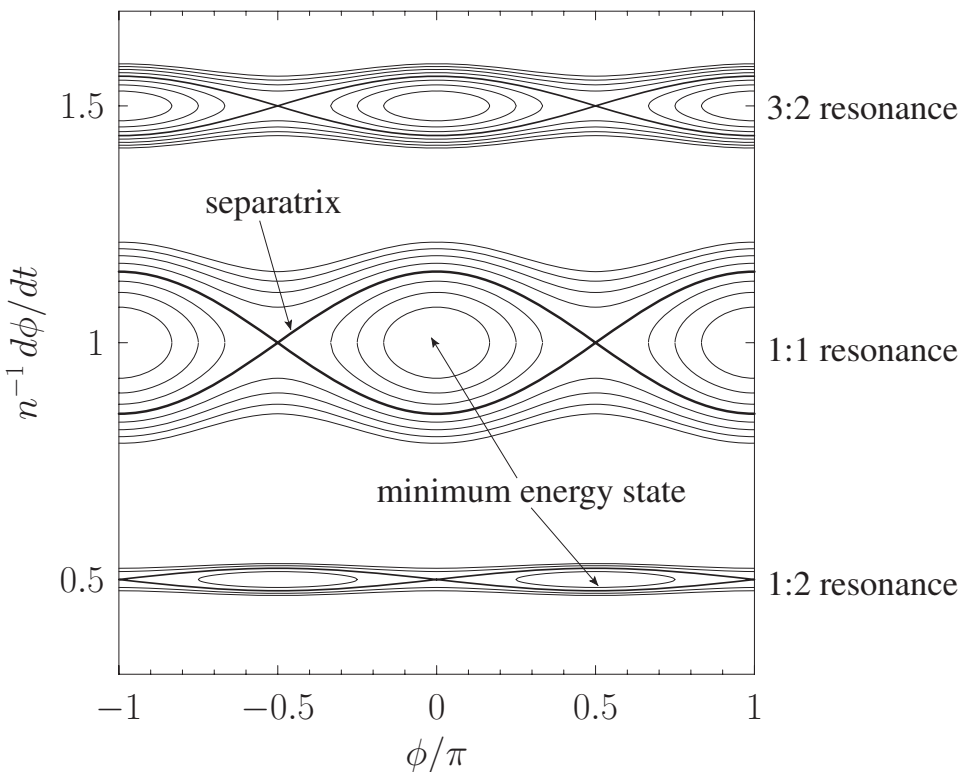


**Fig. 7.9** Contours of  $\mathcal{E}$ , for  $-1 \leq \mathcal{E} \leq 2$ , plotted in  $\phi, n^{-1} d\phi/dt$  space for the 1:2, 1:1, and 3:2 spin-orbit resonances. The contours are calculated with  $\alpha = 0.15$  and  $e = 0.05$ .

Figure 7.9 shows contours of  $\mathcal{E}$  plotted in  $\phi, n^{-1} d\phi/dt$  space for the 1:2, 1:1, and 3:2 spin-orbit resonances. These contours are calculated from Equations (7.174)–(7.176) by using  $\alpha = 0.15$  and  $e = 0.05$ . It can be seen that the contours shown in Figure 7.9 are very similar to the surface of section curves displayed in Figure 7.8—at least, in the vicinity of the resonances. This suggests that the analytic expressions in Equations (7.174)–(7.176) can be used to efficiently map closed surface of section curves in the vicinity of the 1:1, 1:2, and 3:2 spin-orbit resonances. Moreover, it is clear from these expressions that solutions to Equation (7.165) are effectively trapped on such curves. This implies that a solution initially close to (say) a 1:1 resonance will remain close to this resonance indefinitely.

For a given spin-orbit resonance, there exists a *separatrix*, corresponding to the  $\mathcal{E} = 1$  contour, dividing contours that span the whole range of  $\phi$  values from those that only span a restricted range of  $\phi$  values. (See Figure 7.9.) The former contours are characterized by  $\mathcal{E} > 1$ , whereas the latter are characterized by  $\mathcal{E} < 1$ . As the energy integral,  $\mathcal{E}$ , is reduced below the critical value  $\mathcal{E} = 1$ , the range of allowed values of  $\phi$  becomes narrower and narrower. Eventually, when  $\mathcal{E}$  attains its minimum possible value (i.e.,  $\mathcal{E} = -1$ ),  $\phi$  is constrained to take a fixed value. This situation corresponds to an exact spin-orbit resonance. For the case of the 1:1 resonance, the minimum energy state corresponds to  $\phi = 0, \pm\pi$  and  $n^{-1} d\phi/dt = 1$ , which implies that, at the exact

resonance, the moon's  $x$ -axis points directly toward (or away from) the planet at the time of pericenter passage. Because we previously assumed that  $\mathcal{I}_{yy} > \mathcal{I}_{xx}$ , which means that the moon is more elongated in the  $x$ -direction than in the  $y$ -direction, it follows that the long axis (in the  $x$ - $y$  plane) is directed toward the planet each time the moon passes through its pericenter. In this respect, the 3:2 resonance is similar to the 2:1 resonance. However, for a moon with a low-eccentricity orbit locked in a 1:1 spin-orbit resonance, the  $x$ -axis always points in the general vicinity of the planet, even when the moon is far from its pericenter. The same is not true for a moon trapped in a 3:2 resonance. For the case of the 1:2 resonance, the minimum energy state corresponds to  $\phi = \pm\pi/2$  and  $n^{-1} d\phi/dt = 1/2$ , which implies that, at the exact resonance, the moon's  $y$ -axis points directly toward (or away from) the planet at the time of pericenter passage. In other words, the short axis (in the  $x$ - $y$  plane) is directed toward the planet each time the moon passes through its pericenter.

It can be seen from Equations (7.174)–(7.176) that the *resonance widths* (i.e., maximum extent, in the  $n^{-1} d\phi/dt$  direction, of the eyelike structure enclosed by the separatrix) of the 1:1, 1:2, and 3:2 spin-orbit resonances are  $2\alpha$ ,  $\sqrt{2e}\alpha$ , and  $\sqrt{14e}\alpha$ , respectively. As long as these widths are significantly less than the interresonance spacing (which is 1/2), the three resonances remain relatively widely separated and are thus distinct from one another. A rough criterion for the overlap of the 1:1 and 3:2 resonances is

$$\alpha > \frac{1}{2 + \sqrt{14e}}. \quad (7.177)$$

The best example of a celestial body trapped in a 3:2 spin-orbit resonance is the planet Mercury, whose spin period is 58.65 days, and whose orbital period is  $87.97 = 1.5 \times 58.65$  days (Yoder 1995). Note that Mercury's axial tilt (with respect to the normal to its orbital plane) is only  $2'$  (Margot et al. 2007). In other words, Mercury is effectively rotating about an axis that is directed normal to its orbital plane, in accordance with our earlier assumption. It is thought that Mercury was originally spinning faster than at present, but that its spin rate was gradually reduced by the tidal de-spinning effect of the Sun (see Section 5.7), until it fell into a 3:2 spin-orbit resonance. As we have seen, once established, such a resonance is maintained by the locking torque exerted by the Sun on Mercury because of the latter body's small permanent asphericity. However, this is possible only because, close to the resonance, the locking torque exceeds the de-spinning torque.

The best example of a celestial body trapped in a 1:1 spin-orbit resonance is the Moon, whose spin and orbital periods are both 27.32 days. The Moon's axial tilt (with respect to the normal to its orbital plane) is  $1.59^\circ$ . In other words, the Moon is rotating about an axis that is (almost) normal to its orbital plane, in accordance with our previous assumption. Like Mercury, it is thought that the Moon was originally spinning faster than at present, but that its spin rate was gradually reduced by tidal de-spinning until it fell into a 1:1 spin-orbit resonance. This resonance is maintained by the locking torque exerted by the Earth on the Moon because of the latter body's small permanent asphericity, rather than by tidal effects, as (when the eccentricity of the lunar orbit is taken into

account) tidal effects alone would actually cause the moon's spin rate to exceed its mean orbital rotation rate by about 3 percent (Murray and Dermott 1999).

Consider a moon whose spin state is close to an exact 1:1 spin-orbit resonance. According to the full (i.e., nonaveraged) equation of motion, Equation (7.169),

$$\frac{d^2\gamma}{dt^2} + n_0^2 \gamma \simeq 2e n_0^2 \sin(nt), \quad (7.178)$$

where we have assumed that  $|\gamma| \ll 1$  (because the moon is close to the exact resonance) and have also neglected terms of order  $e\gamma$  with respect to unity. The preceding equation has the standard solution

$$\gamma = -\gamma_0 \sin(n_0 t - \varphi_0) - 2e \frac{n_0^2}{n^2 - n_0^2} \sin M, \quad (7.179)$$

where  $\gamma_0$  and  $\varphi_0$  are arbitrary. This expression is more conveniently written

$$\gamma = -\gamma_0 \sin(n_0 t - \varphi_0) - 2e \frac{\alpha^2}{1 - \alpha^2} \sin M. \quad (7.180)$$

From Equations (7.157), (7.160), and (7.168), we have

$$\eta \simeq 2e \sin M - \gamma, \quad (7.181)$$

which implies that

$$\eta \simeq 2e \sin M + \gamma_0 \sin(n_0 t - \varphi_0) + 2e \frac{\alpha^2}{1 - \alpha^2} \sin M. \quad (7.182)$$

Here,  $\eta$  is the angle subtended between the moon's  $x$ -axis and the line joining the center of the moon to the planet. (See Figure 7.7.) According to the preceding equation, this angle *librates* (i.e., oscillates). The first term on the right-hand side of the preceding expression describes so-called *optical libration* (in longitude). This is merely a perspective effect due to the eccentricity of the moon's orbit; it does not imply any irregularity in the moon's axial spin rate. The final two terms describe so-called *physical libration* (in longitude) and are associated with real irregularities in the moon's spin rate. To be more exact, the first of these terms describes *free libration* (in longitude), whereas the second describes *forced libration* (in longitude). Optical libration causes an oscillation in  $\eta$  whose period matches the moon's orbital period, whose amplitude (in radians) is  $2e$ , and whose phase is such that  $\eta = 0$  as the moon passes through its pericenter. Forced libration causes a similar oscillation of much smaller amplitude (assuming that  $\alpha \ll 1$ ). Free libration, on the other hand, causes an oscillation in  $\eta$  whose period is  $\alpha^{-1}$  times the moon's orbital period, and whose amplitude and phase are arbitrary.

Consider the Moon, whose spin state is close to a 1:1 spin-orbit resonance. According to data from the Lunar Prospector probe (Konopliv et al. 1998),

$$\frac{\mathcal{I}_{yy} - \mathcal{I}_{xx}}{\mathcal{I}_{zz}} = 2.279 \times 10^{-4}, \quad (7.183)$$

which implies that

$$\alpha = 2.615 \times 10^{-2}. \quad (7.184)$$

Hence, given that the Moon's orbital period is 27.322 days (i.e., a sidereal month), the predicted free libration period is 2.86 years. Because of the comparatively rapid precession of the Moon's perigee (which completes a full circuit about the Earth every 8.85 years—see Chapter 10), the expected period of both optical and forced libration (in longitude) is 27.555 days (i.e., an anomalistic month). Moreover, the predicted amplitudes of these librations are  $6.5^\circ$  [when evaluated up to  $\mathcal{O}(e^2)$ ], and  $15.8''$ , respectively. Optical libration (in longitude) has been observed for hundreds of years and does indeed have the characteristics described earlier. Furthermore, despite having an amplitude that is a thousand times less than that of optical libration, the forced libration (in longitude) of the Moon (due to the eccentricity of the lunar orbit) is measurable by means of laser ranging. The observed period and amplitude are 27.555 days and  $16.8''$ , respectively (Williams and Dickey 2003), and are in good agreement with the above predictions. Finally, a free libration (in longitude) mode of the Moon with a period of 2.87 years and an amplitude of  $1.87''$  has been observed via laser ranging (Jin and Li 1996). The period of this libration is, thus, in good agreement with our analysis. Note that, since the Moon's orbit has significant non-Keplerian elements, due to the perturbing action of the Sun, the Moon's forced libration (in longitude) also has important non-Keplerian elements. (See Exercise 10.7.) Furthermore, the Moon also possesses free and forced modes of libration in latitude. (See Section 7.12.)

The forced libration of the Moon is a tiny effect because of the Moon's relatively small departures from sphericity. There exist other moons in the solar system, however, that are locked in a 1:1 spin-orbit resonance (like the Moon) and whose departures from sphericity are substantial. For such moons, forced libration can attain quite large amplitudes. A prime example is the Martian moon Phobos. The shape of this moon, which is highly irregular (see Figure 2.2), has been measured to high precision by the Mars Express probe, allowing the computation of the relative magnitudes of its principal moments of inertia (on the assumption that the moon is homogeneous). According to this calculation (Wilner et al. 2010),

$$\frac{\mathcal{I}_{yy} - \mathcal{I}_{xx}}{\mathcal{I}_{zz}} = 0.129, \quad (7.185)$$

which implies that

$$\alpha = 0.623. \quad (7.186)$$

Because the observed eccentricity of Phobos' orbit is  $e = 0.0151$  (Yoder 1995), the predicted amplitude of its forced physical libration is  $1.1^\circ$ . The measured amplitude is  $1.2^\circ$  (Wilner et al. 2010). Note that the  $\alpha$  and  $e$  values for Phobos satisfy the resonance overlap criterion in Equation (7.177). Figure 7.10 shows a surface of section plot for Phobos. It can be seen that resonance overlap leads to the destruction of many of the closed curves that are a feature of Figure 7.8. Nevertheless, some closed curves remain intact, especially in the vicinity of the 1:1 spin-orbit resonance, that is, around  $\phi = 0$ ,  $\pm\pi$ , and  $n^{-1} d\phi/dt = 1$ . Consequently, it is possible for Phobos to remain close to a 1:1 spin-orbit resonant state for an indefinite period of time.

The most extreme example of spin-orbit coupling in the solar system occurs in Hyperion, which is a small moon of Saturn. Hyperion has a highly irregular shape, with an

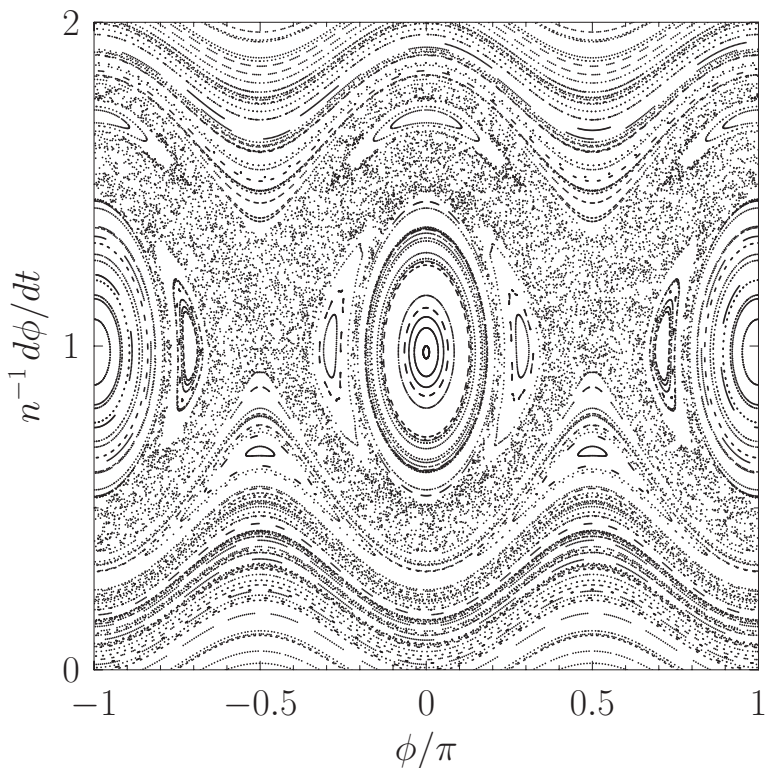


**Fig. 7.10** Surface of section plot for various solutions of Equation (7.165) with the Phobos-like parameters  $\alpha = 0.623$  and  $e = 0.0151$ .

asphericity parameter of

$$\alpha \simeq 0.89 \quad (7.187)$$

(calculated on the assumption that Hyperion is homogeneous), and is in a fairly eccentric orbit of eccentricity

$$e = 0.123 \quad (7.188)$$

(Thomas et al. 1995). Hence, Hyperion easily satisfies the resonance overlap criterion in Equation (7.177). Figure 7.11 shows a surface of section plot for Hyperion. It can be seen that resonance overlap leads to the complete destruction of all the closed curves associated with the 1:1 spin-orbit resonance. This would seem to imply that Hyperion cannot remain trapped in a 1:1 resonance for any appreciable length of time. Figure 7.12 shows the time evolution of a solution of Equation (7.165), with Hyperion-like values of  $\alpha$  and  $e$ , that starts off in an exact 1:1 spin-orbit resonance. If the solution were to stay close to the resonant state, the angle  $\gamma$ —and, hence,  $\sin \gamma$ —would remain close to zero. It can be seen, from the figure, that this is not the case. In fact,  $\sin \gamma$  quickly becomes of order unity, indicating a strong deviation from the resonant state. Moreover,  $\sin \gamma$ —and, hence,  $\gamma$  itself—subsequently varies in a markedly irregular manner. The time variation

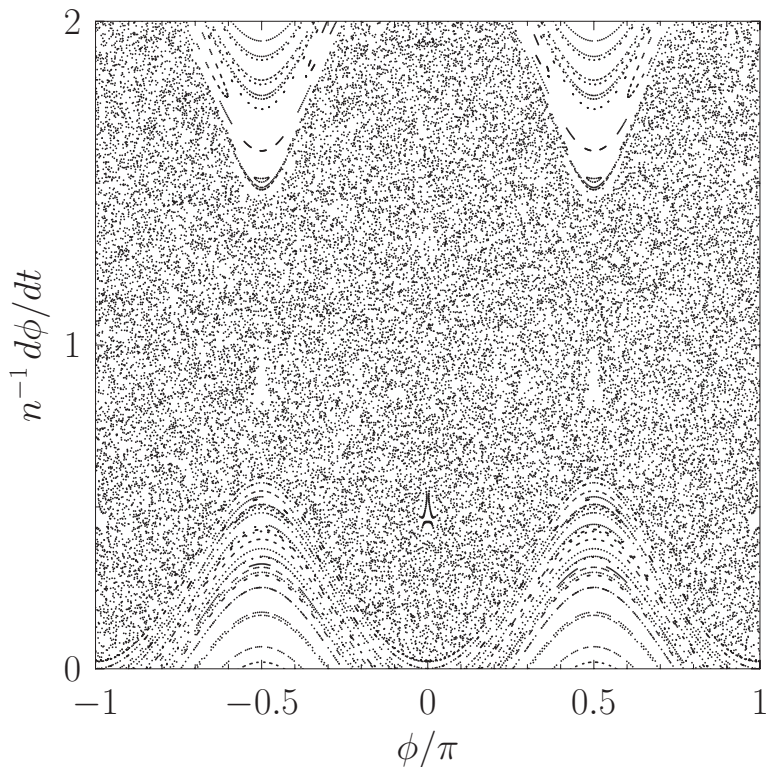


**Fig. 7.11** Surface of section plot for various solutions of Equation (7.165) with the Hyperion-like parameters  $\alpha = 0.89$  and  $e = 0.123$ .

of  $\gamma$  is in fact *chaotic*: that is, it is quasi-random, never repeats itself, and exhibits extreme sensitivity to initial conditions (Strogatz 2001). This suggests that Hyperion is spinning in a chaotic manner. Data from the Voyager 2 probe seem to confirm that this is indeed the case (Black et al. 1995). (Note, however, that Hyperion's spinning motion involves large chaotic variations in its axial tilt that are not taken into account in our analysis.)

## 7.12 Cassini's laws

Consider Figure 7.13. Here,  $M$ ,  $E$ , and  $N$  represent the center of the Moon, the center of the Earth, and the north ecliptic pole, respectively. Moreover,  $MZ$  is the instantaneous normal to the Moon's equatorial plane, and  $MP$  the instantaneous normal to the Moon's orbital plane. Let  $\mathbf{e}$ ,  $\zeta$ ,  $\nu$ , and  $\mathbf{p}$  be unit vectors parallel to  $ME$ ,  $MZ$ ,  $MN$ , and  $MP$ , respectively. The *fixed* angle,  $I = 5.16^\circ$ , subtended between the directions of  $\mathbf{p}$  and  $\nu$ , represents the fixed inclination of the Moon's orbital plane to the ecliptic plane. Furthermore, as is well known, because of the perturbing action of the Sun, the normal to the Moon's orbital plane,  $\mathbf{p}$ , precesses about the normal to the ecliptic plane,  $\nu$ , in

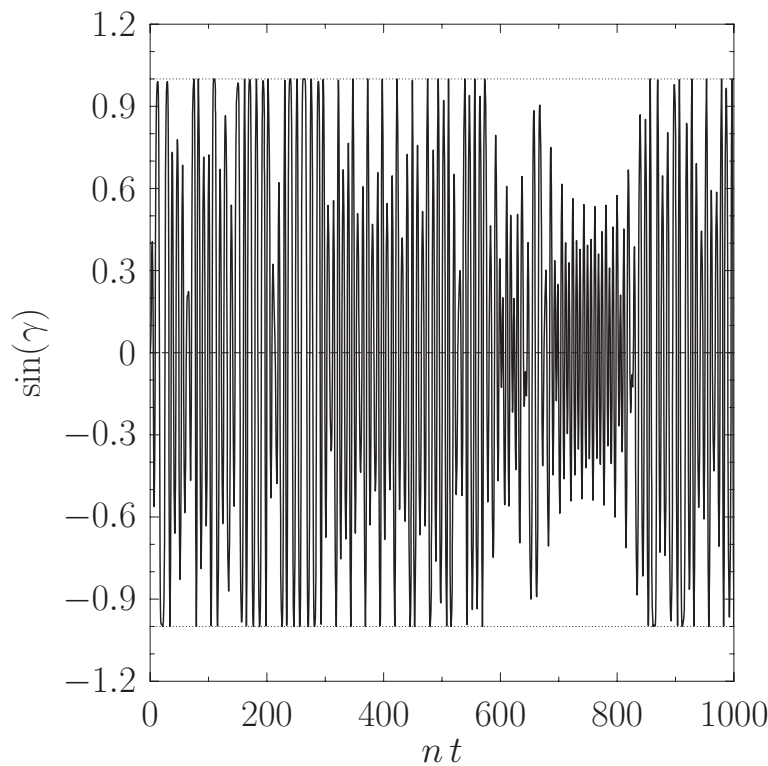


**Fig. 7.12** Solution of Equation (7.165) with the Hyperion-like parameters  $\alpha = 0.89$  and  $e = 0.123$ . The initial conditions are  $\phi = 0$  and  $n^{-1} d\phi/dt = 1$ . Here,  $\gamma = \phi - nt$ .

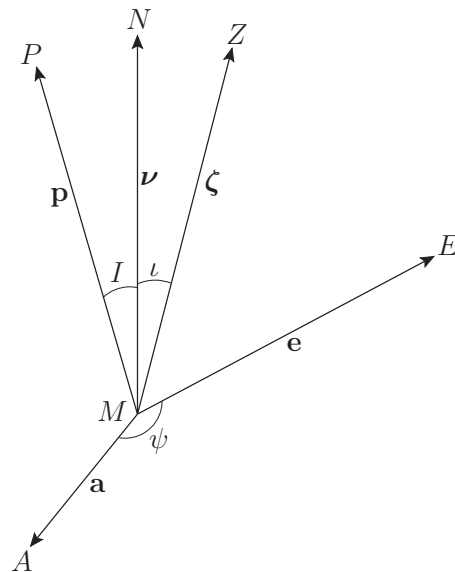


**Fig. 7.13** Geometry of Cassini's laws.

the opposite sense to the Moon's orbital motion, such that it completes a full circuit every 18.6 years. (See Chapter 10.) Recall that precession in the opposite sense to orbital motion is usually termed *regression*.

In 1693, the astronomer Gian Domenico Cassini (1625–1712) formulated a set of empirical laws that succinctly describe the Moon's axial rotation. According to these laws:

1. The Moon spins at a *uniform* rate that matches its mean orbital rotation rate.
2. The normal to the Moon's equatorial plane subtends a *fixed* angle,  $\iota = 1.59^\circ$ , with the normal to the ecliptic plane.
3. The normal to the Moon's equatorial plane, the normal to the Moon's orbital plane, and the normal to the ecliptic plane are *coplanar* vectors that are oriented such that the latter vector lies between the other two.

Law 1 effectively states that the Moon is locked in a 1:1 spin-orbit resonance. (See Section 7.11.) Let the  $x$ -,  $y$ -, and  $z$ -axes be the Moon's principal axes of rotation, and let  $\mathcal{I}_{xx}$ ,  $\mathcal{I}_{yy}$ , and  $\mathcal{I}_{zz}$  be the corresponding principal moments of inertia. Furthermore, let us label the principal axes such that the Moon's equatorial plane corresponds to the  $x$ – $y$  plane, the normal to the equatorial plane corresponds to the  $z$ -axis, and  $\mathcal{I}_{yy} > \mathcal{I}_{xx}$ . In this case, as we saw in the previous section, a 1:1 spin-orbit resonant state is such that the Moon's  $x$ -axis always points approximately in the direction of the Earth: that is,  $\mathbf{e}$  is almost parallel to the  $x$ -axis.

Law 2 states that the angle,  $\iota$ , subtended between  $\zeta$  and  $\nu$  is fixed. Moreover, because the angles  $I$  and  $\iota$  are both small (when expressed in radians), we deduce that the vectors  $\nu$  and  $\mathbf{p}$  are almost parallel to  $\zeta$ .

Law 3 states that the vectors  $\zeta$ ,  $\nu$ , and  $\mathbf{p}$  all lie in the same plane, with  $\zeta$  and  $\mathbf{p}$  on opposite sides of  $\nu$ . In other words, as the normal to the Moon's orbital plane,  $\mathbf{p}$ , regresses about the normal to the ecliptic plane,  $\nu$ , the normal to the Moon's equatorial plane,  $\zeta$ , regresses at the same rate, such that  $\zeta$  is always directly opposite  $\mathbf{p}$  with respect to  $\nu$ .

Cassini's first law was accounted for in the previous section. The ultimate aim of this section is to account for Cassini's second and third laws. Our approach is largely based on that of Danby (1992). To simplify the analysis, we shall assume that the Moon orbits around the Earth, at the uniform angular velocity,  $n$ , in a circular orbit of major radius  $a$ . When expressed in terms of the  $x$ ,  $y$ ,  $z$  coordinate system,  $\zeta = (0, 0, 1)$ . Furthermore, because the unit vectors  $\nu$  and  $\mathbf{p}$  are almost parallel to  $\zeta$ , we can write

$$\nu \simeq (\nu_x, \nu_y, 1) \quad (7.189)$$

and

$$\mathbf{p} \simeq (p_x, p_y, 1), \quad (7.190)$$

where  $|\nu_x|, |\nu_y|, |p_x|, |p_y| \ll 1$ . Similarly, because the unit vector  $\mathbf{e}$  is almost parallel to the  $x$ -axis, we have

$$\mathbf{e} \simeq (1, e_y, e_z), \quad (7.191)$$

where  $|e_y|, |e_z| \ll 1$ . The position vector,  $\mathbf{r} = (x, y, z)$ , of the center of the Earth with respect to the center of the Moon is written

$$\mathbf{r} = a \mathbf{e}. \quad (7.192)$$

Finally, given Cassini's first law, and assuming that the Moon's spin axis is almost parallel to the  $z$ -axis, we find that the Moon's spin angular velocity takes the form

$$\boldsymbol{\omega} = n \mathbf{w}. \quad (7.193)$$

Here,  $\mathbf{w}$  is a unit vector such that

$$\mathbf{w} \approx (w_x, w_y, 1), \quad (7.194)$$

where  $|w_x|, |w_y| \ll 1$ .

According to Equations (7.149), (7.150), (7.152), and (7.153),

$$\dot{\omega}_x + \sigma \omega_y \omega_z = 3n^2 \sigma \frac{y z}{a^2} \quad (7.195)$$

and

$$\dot{\omega}_y - \tau \omega_x \omega_z = -3n^2 \tau \frac{x z}{a^2}, \quad (7.196)$$

because  $r = a$  and  $G m_p = n^2 a^3$ . Here,

$$\sigma = \frac{\mathcal{I}_{zz} - \mathcal{I}_{yy}}{\mathcal{I}_{xx}} \quad (7.197)$$

and

$$\tau = \frac{\mathcal{I}_{zz} - \mathcal{I}_{xx}}{\mathcal{I}_{yy}}. \quad (7.198)$$

Note that  $|\sigma|, |\tau| \ll 1$  because the Moon is almost spherically symmetric. To second order in small quantities, Equations (7.195) and (7.196) yield

$$n^{-1} \dot{w}_x + \sigma w_y \approx 0 \quad (7.199)$$

and

$$n^{-1} \dot{w}_y - \tau w_x \approx -3 \tau e_z, \quad (7.200)$$

where use has been made of Equations (7.191)–(7.194).

The unit vector  $\mathbf{v}$  is *stationary* in an inertial frame whose coordinate axes are fixed with respect to distant stars. Hence, in the  $x, y, z$  body frame, which rotates with respect to the aforementioned fixed frame at the angular velocity  $\boldsymbol{\omega}$ , we have (see Section 5.2)

$$\frac{d\mathbf{v}}{dt} + \boldsymbol{\omega} \times \mathbf{v} = \mathbf{0}. \quad (7.201)$$

It follows, from Equations (7.189), (7.193), and (7.194), that

$$w_x \approx n^{-1} \dot{v}_y + v_x \quad (7.202)$$

and

$$w_y \approx -n^{-1} \dot{v}_x + v_y. \quad (7.203)$$

These expressions can be combined with Equations (7.199) and (7.200) to give

$$n^{-2} \ddot{v}_x - (1 - \tau) n^{-1} \dot{v}_y + \tau v_x \simeq 3 \tau e_z \quad (7.204)$$

and

$$n^{-2} \ddot{v}_y + (1 - \sigma) n^{-1} \dot{v}_x + \sigma v_y \simeq 0. \quad (7.205)$$

It now remains to express  $e_z$  in terms of  $v_x$  and  $v_y$ .

By definition,  $\mathbf{p}$  is normal to  $\mathbf{e}$ , since the vector  $\mathbf{e}$  lies in the plane of the Moon's orbit. Hence, according to Equations (7.190) and (7.191),

$$\mathbf{p} \cdot \mathbf{e} \simeq p_x + e_z = 0, \quad (7.206)$$

which implies that

$$e_z \simeq -p_x. \quad (7.207)$$

Let  $A$  be the ascending node of the Earth's apparent orbit about the Moon (which implies that  $A$  is the descending node of the Moon's actual orbit about the Earth), and let  $\mathbf{a}$  be a unit vector parallel to  $\mu A$ . (See Figure 7.13 and Section 3.12.) By definition,  $\mathbf{a}$  is normal to both  $\mathbf{p}$  and  $\mathbf{v}$ . In fact, we can write

$$\mathbf{a} = \frac{\mathbf{v} \times \mathbf{p}}{\sin I}, \quad (7.208)$$

where  $I$  is the angle subtended between the vectors  $\mathbf{p}$  and  $\mathbf{v}$ . It follows from Equations (7.189) and (7.190), and the fact that  $I$  is small, that

$$\mathbf{a} \simeq I^{-1} (v_y - p_y, p_x - v_x, v_x p_y - v_y p_x). \quad (7.209)$$

Now,

$$\mathbf{a} \cdot \mathbf{e} = \cos \psi \quad (7.210)$$

and

$$\mathbf{a} \times \mathbf{e} \cdot \mathbf{p} = \sin \psi, \quad (7.211)$$

where  $\psi$  is the angle subtended between  $\mathbf{a}$  and  $\mathbf{e}$ . (See Figure 7.13.) Thus, Equations (7.190), (7.191), and (7.209) yield

$$v_x = p_x + I \sin \psi, \quad (7.212)$$

$$v_y = p_y + I \cos \psi, \quad (7.213)$$

and

$$\mathbf{a} \simeq (\cos \psi, -\sin \psi, v_y \sin \psi - v_x \cos \psi). \quad (7.214)$$

In fact,  $\psi$  is the longitude of the Earth relative to the ascending node of its apparent orbit around the Moon. It follows that

$$\psi = (n + g)t, \quad (7.215)$$

where  $g$  is the uniform regression rate of the Earth's apparent ascending node (which is the same as the regression rate of the true ascending node of the Moon's orbit around the Earth). Here, for the sake of simplicity, we have assumed that the Earth passes through

its apparent ascending node at time  $t = 0$ . Hence, Equations (7.204), (7.205), (7.207), (7.212), and (7.215) can be combined to give

$$n^{-2} \ddot{v}_x - (1 - \tau) n^{-1} \dot{v}_y + 4 \tau v_x \simeq 3 \tau I \sin[(n + g) t] \quad (7.216)$$

and

$$n^{-2} \ddot{v}_y + (1 - \sigma) n^{-1} \dot{v}_x + \sigma v_y \simeq 0. \quad (7.217)$$

The previous two equations govern the Moon's physical libration in *latitude*. As is the case for libration in longitude, there are both free and forced modes. The free modes satisfy

$$n^{-2} \ddot{v}_x - (1 - \tau) n^{-1} \dot{v}_y + 4 \tau v_x \simeq 0 \quad (7.218)$$

and

$$n^{-2} \ddot{v}_y + (1 - \sigma) n^{-1} \dot{v}_x + \sigma v_y \simeq 0. \quad (7.219)$$

Let us search for solutions of the form

$$v_x(t) = \hat{v}_x \sin(st - \phi) \quad (7.220)$$

and

$$v_y(t) = \hat{v}_y \cos(st - \phi), \quad (7.221)$$

where  $\hat{v}_x, \hat{v}_y, \phi$  are constants. It follows that

$$\frac{\hat{v}_y}{\hat{v}_x} = \frac{s^2 - 4\tau}{(1 - \tau)s} = \frac{(1 - \sigma)s}{s^2 - \sigma}. \quad (7.222)$$

Given that  $|\sigma|$  and  $|\tau|$  are both small compared to unity, two independent free libration modes can be derived from the preceding expression. The first mode is such that  $s \simeq 1 + 3\tau/2$  and  $\hat{v}_y/\hat{v}_x \simeq 1 - 3\tau/2$ , whereas the second is such that  $s \simeq 2\sqrt{\sigma\tau}$  and  $\hat{v}_y/\hat{v}_x \simeq -2\sqrt{\tau/\sigma}$ . In the Moon's body frame, these modes cause the normal to the ecliptic plane,  $\nu = (v_x, v_y, 1)$ , to precess about the normal to the Moon's equatorial plane,  $\zeta = (0, 0, 1)$ , in such a manner that

$$v_x \simeq A_1 \sin(\omega_1 t - \phi_1) + A_2 \sin(\omega_2 t - \phi_2) \quad (7.223)$$

and

$$v_y \simeq K_1 A_1 \cos(\omega_1 t - \phi_1) + K_2 A_2 \cos(\omega_2 t - \phi_2), \quad (7.224)$$

where  $\omega_1 \simeq n(1 + 3\tau/2)$ ,  $\omega_2 \simeq 2n\sqrt{\sigma\tau}$ ,  $K_1 \simeq 1 - 3\tau/2$ ,  $K_2 \simeq -2\sqrt{\tau/\sigma}$ , and the constants  $A_1, A_2, \phi_1, \phi_2$  are arbitrary. The observed values of  $n$ ,  $\sigma$ , and  $\tau$  are  $13.1764^\circ$  per day,  $4.0362 \times 10^{-4}$ , and  $6.3149 \times 10^{-4}$ , respectively (Konopliv et al. 1998). Thus, it follows that  $\omega_1 = 13.1889^\circ$  day,  $\omega_2 = 1.3304 \times 10^{-2}^\circ$  day,  $K_1 = 0.9991$ , and  $K_2 = -2.5017$ . In the body frame, the first mode causes  $\nu$  to regress about  $\zeta$  with a period of 27.2957 days, whereas the second mode causes  $\nu$  to precess about  $\zeta$  with a period of 74.1 years. Both these modes of libration have been detected by means of lunar laser ranging. The measured amplitude of the first mode is  $A_1 = 0.37''$ , whereas that of the second mode is  $A_2 = 3.25''$  (Jin and Li 1996). Incidentally, the second mode is very

similar in nature to the Chandler wobble of the Earth. (See Section 7.8.) Note that if  $\sigma$  and  $\tau$  were of opposite sign—that is, if  $\mathcal{I}_{zz}$  were intermediate between  $\mathcal{I}_{xx}$  and  $\mathcal{I}_{yy}$ —the second mode of libration would grow exponentially in time, rather than oscillate at a constant amplitude: in other words, the Moon’s spin state would be unstable. In fact, the Moon’s principal axes of rotation are oriented such that  $\mathcal{I}_{zz} > \mathcal{I}_{yy} > \mathcal{I}_{xx}$ , which ensures that the Moon spins in a stable manner.

Let us now search for forced solutions of Equations (7.216) and (7.217) of the form

$$\nu_x = \hat{\nu}_x \sin[(n + g)t] \quad (7.225)$$

and

$$\nu_y = \hat{\nu}_y \cos[(n + g)t], \quad (7.226)$$

where  $\hat{\nu}_x$ ,  $\hat{\nu}_y$  are constants. It follows that

$$\left[4\tau - (1 + g/n)^2\right]\hat{\nu}_x + (1 - \tau)(1 + g/n)\hat{\nu}_y \simeq 3\tau I \quad (7.227)$$

and

$$(1 - \sigma)(1 + g/n)\hat{\nu}_x + \left[\sigma - (1 + g/n)^2\right]\hat{\nu}_y \simeq 0. \quad (7.228)$$

Hence, recalling that  $\sigma$ ,  $\tau$ , and  $g/n$  are all small compared to unity, we obtain the following mode of forced libration:

$$\frac{\hat{\nu}_y}{\hat{\nu}_x} \simeq 1 - \frac{g}{n} \quad (7.229)$$

and

$$\hat{\nu}_x \simeq \frac{3\tau I}{3\tau - g/n}. \quad (7.230)$$

In the Moon’s body frame, this mode causes the vectors  $\nu$  and  $\mathbf{p}$  to regress about  $\zeta$  (i.e., the  $z$ -axis) in such a manner that

$$\nu \simeq (-\iota \sin \psi, -\iota \cos \psi, 1) \quad (7.231)$$

and

$$\mathbf{p} \simeq (-(I + \iota) \sin \psi, -(I + \iota) \cos \psi, 1), \quad (7.232)$$

where

$$\iota = \frac{3\tau I}{2g/n - 3\tau}, \quad (7.233)$$

and use has been made of Equations (7.212), (7.213), and (7.215). Because the observed values of  $I$ ,  $\tau$ , and  $g/n$  are  $I = 5.16^\circ$ ,  $\tau = 6.3149 \times 10^{-4}$ , and  $g = 4.0185 \times 10^{-3}$  (Konopliv et al. 1998; Yoder 1995), we deduce that

$$\iota = 1.59^\circ. \quad (7.234)$$

According to Equation (7.231),  $\nu$  regresses around  $\zeta$ , with a period of 27.2123 days (i.e., a draconic month), in such a manner that  $\nu$  subtends a *fixed* angle of  $\iota = 1.59^\circ$  with respect to  $\zeta$ . This accounts for Cassini’s second law. According to Equation (7.232),  $\mathbf{p}$  simultaneously regresses around  $\zeta$ , with the same period, in such a manner that  $\zeta \cdot \nu \times \mathbf{p} = 0$ .

In other words, the three vectors  $\zeta$ ,  $\nu$ , and  $\mathbf{p}$  always lie in the same plane. Moreover, it is clear that  $\nu$  is intermediate between  $\zeta$  and  $\mathbf{p}$ . This accounts for Cassini's third law. The angle  $I' = I + \iota$ , subtended between  $\zeta$  and  $\mathbf{p}$ , which is also the angle of inclination between the Moon's equatorial and orbital planes, takes the fixed value

$$I' = \frac{2(g/n)I}{2g/n - 3\tau} = 6.75^\circ. \quad (7.235)$$

This angle would be zero in the absence of any regression of the Moon's orbital ascending node (i.e., if  $g/n$  were zero). In other words, the nonzero angle of inclination between the Moon's equatorial and orbital planes is a direct consequence of this regression, which is ultimately due to the perturbing action of the Sun. Because the regression of the Moon's orbital ascending node is also responsible for the forced nutation of the Earth's axis of rotation (see Section 7.10), it follows that this nutation is closely related to the forced inclination between the Moon's equatorial and orbital planes.

## Exercises

- 7.1** Let  $\mathbf{e}_z'$ ,  $\mathbf{L}$ , and  $\boldsymbol{\omega}$  be the symmetry axis, the angular momentum vector, and the angular velocity vector, respectively, of a rotating body with an axis of symmetry. Demonstrate that these three vectors are coplanar.
- 7.2** Verify Equations (7.50) and (7.51).
- 7.3** A rigid body having an axis of symmetry rotates freely about a fixed point under no torques. If  $\alpha$  is the angle between the symmetry axis and the instantaneous axis of rotation, show that the angle between the axis of rotation and the invariable line (the  $\mathbf{L}$  vector) is
- $$\tan^{-1} \left[ \frac{(\mathcal{I}_{\parallel} - \mathcal{I}_{\perp}) \tan \alpha}{\mathcal{I}_{\parallel} + \mathcal{I}_{\perp} \tan^2 \alpha} \right],$$
- where  $\mathcal{I}_{\parallel}$  (the moment of inertia about the symmetry axis) is greater than  $\mathcal{I}_{\perp}$  (the moment of inertia about an axis normal to the symmetry axis). (From Fowles and Cassiday 2005.)
- 7.4** Because the greatest value of  $\mathcal{I}_{\parallel}/\mathcal{I}_{\perp}$  is 2 (symmetrical lamina), show from the previous result that the angle between the angular velocity and angular momentum vectors cannot exceed  $\tan^{-1}(1/\sqrt{8}) \approx 19.5^\circ$ . Find the corresponding value of  $\alpha$ . (Modified from Fowles and Cassiday 2005.)
- 7.5** A thin uniform rod of length  $l$  and mass  $m$  is constrained to rotate with constant angular velocity  $\omega$  about an axis passing through the center of the rod, and making an angle  $\alpha$  with the rod. Show that the angular momentum about the center of the rod is perpendicular to the rod and is of magnitude  $(ml^2\omega/12)\sin\alpha$ . Show that the torque is perpendicular to both the rod and the angular momentum vector and is of magnitude  $(ml^2\omega^2/12)\sin\alpha\cos\alpha$ . (From Fowles and Cassiday 2005.)
- 7.6** A thin uniform disk of radius  $a$  and mass  $m$  is constrained to rotate with constant angular velocity  $\omega$  about an axis passing through its center, and making an angle

$\alpha$  with the normal to the disk. Find the angular momentum about the center of the disk, as well as the torque acting on the disk.

- 7.7** A freely rotating rigid body has principal moments of inertia such that  $\mathcal{I}_{zz} > \mathcal{I}_{yy} > \mathcal{I}_{xx}$ .
- Demonstrate that the rotational energy of the body attains its maximum and minimum values (at fixed  $\omega$ ) when the body rotates about the  $z$ - and the  $x$ -axes, respectively.
  - Demonstrate, from Euler's equations, that the rotational state is stable to small perturbations when the body rotates about either the  $x$ -axis or the  $z$ -axis, but is unstable when it rotates about the  $y$ -axis.
- 7.8** The length of the *mean sidereal year*, which is defined as the average time required for the Sun to (appear to) complete a full orbit around the Earth, relative to the fixed stars, is 365.25636 days (Yoder 1995). The *mean tropical year* is defined as the average time interval between successive vernal equinoxes. Demonstrate that, as a consequence of the precession of the equinoxes, whose period is 25,772 years (Yoder 1995), the length of the mean tropical year is 20.4 minutes shorter than that of the mean sidereal year (i.e., 365.24219 days).
- 7.9** Consider an artificial satellite in a circular orbit of radius  $a$  about the Earth. Suppose that the normal to the plane of the orbit subtends an angle  $I$  with the Earth's axis of rotation. By approximating the orbiting satellite as a uniform ring, demonstrate that the Earth's oblateness causes the plane of the satellite's orbit to precess about the Earth's rotational axis at the approximate rate

$$\frac{3}{2} J_2 n \left( \frac{R}{a} \right)^2 \cos I.$$

Here,  $n$  is the satellite's orbital angular velocity,  $R$  is the Earth's mean radius,  $J_2 = (\mathcal{I}_{\parallel} - \mathcal{I}_{\perp})/(MR^2)$ ,  $M$  is the Earth's mass, and  $\mathcal{I}_{\parallel}$  and  $\mathcal{I}_{\perp}$  are the Earth's parallel and perpendicular (to the rotation axis) moments of inertia. Is the precession in the same sense as the orbital motion, or the opposite sense?

- 7.10** A *Sun-synchronous* satellite is one that always passes over a given point on the Earth at the same local solar time. This is achieved by fixing the precession rate of the satellite's orbital plane such that it matches the rate at which the Sun appears to move against the background of the stars. What orbital altitude above the surface of the Earth would such a satellite need to have in order to fly over all latitudes between 50° N and 50° S? Is the direction of the satellite orbit in the same sense as the Earth's rotation (prograde), or the opposite sense (retrograde)? Note that  $J_2 = 1.083 \times 10^{-3}$  for the Earth (Yoder 1995).
- 7.11** Consider an aspherical moon in a low-eccentricity Keplerian orbit about a spherical planet. Suppose that the moon is locked in a 1:1 spin-orbit resonance. Demonstrate that, to lowest order in the eccentricity, the optical libration of the moon can be accounted for by saying that the moon's long axis (in the orbital plane) always points toward the empty focus of the orbit.